SLAC-PUB-1141
(TH) and (EXP)
October 1972

DIFFRACTION DISSOCIATION[†]

David W. G. S. Leith
Stanford Linear Accelerator Center
Stanford University, Stanford, California 94305

Introduction

This is not a complete review of the diffraction dissociation phenomena, but only a summary, albeit incomplete, of the papers presented to the Conference. A more leisurely and complete discussion of the subject can be found in recent reviews by Kane[1] and Lubatti.[2] I have tried to summarize the data in a coherent picture (no pun intended), by comparing the properties of these inelastic diffractive processes to those of elastic scattering.

What is this diffraction dissociation process we are to discuss? We describe it in terms of the exchange of the Pomeron in the t channel, but since we do not really understand what the Pomeron is, we cannot go much further. We more readily identify the diffraction process by its properties observed in scattering reactions:

1. energy independent cross sections (or only weakly dependent, to factors of log s);
2. particle cross sections about equal to antiparticle cross sections;
3. sharp forward peak in the differential cross section;
4. exchange process characterized by the quantum number of the vacuum in the t-channel (i.e., I=0, C=+1), and the change in J^P during scattering follows the natural spin-parity series, $P(-1)^J$;
5. the spin structure in the scattering seems to be s-channel helicity conserving (SCHC).

When a given reaction exhibits the above characteristics, or most of them, we describe it as a diffractive process and try to interpret it in terms of the exchange of a Pomeron in Regge language. Now one word of warning — it is pretty clear that the Pomeron is not a simple pole. The evidence of the rising K^+p total cross section at Serpukov energies, the relatively flat pp total cross sections through ISR energies, the changes of slope for the pp differential cross section both as a function of s and t — all of these effects warn us that the Pomeron is not a simple Regge pole. However, so warned we proceed to determine from a phenomenological point of view the properties of diffraction dissociation.

The classical reactions to learn of diffraction are:

$$\pi N \to \pi N\,, \qquad KN \to KN\,, \qquad NN \to NN\,, \qquad \gamma N \to \gamma N\,,$$

but in this review we have to deal with their "poor-cousins":

$$\pi N \to (3\pi)N\,, \qquad KN \to (K\pi\pi)N\,, \qquad NN \to (N\pi\pi)N\,, \qquad \gamma N \to (V)N\,.$$

All but the last of these processes involve a change of spin in the diffracting process, and all but the last have no clear resonance signal in the diffracting system,[‡] and as we shall see, all but the last will give us some trouble with our traditional diffraction picture.

In the following sections we will consider the data presented to the Conference on cross sections, differential cross sections, and spin structure for the diffractive processes listed above, and whenever possible compare them to the well known elastic scattering properties.

[†]Work supported by the U. S. Atomic Energy Commission.

[‡]The following discussion does not depend greatly on whether the (3π), $(K\pi\pi)$, $(N\pi\pi)$ final states are resonant or purely some kinematical effect. They seem to be dominated by a single, well defined spin-parity state and form quite specific and identifiably processes. We will be concerned with the dynamics of production in these processes and the phenomenological characteristics of the reactions, independent of the question of the final state phases.

(Invited talk presented at the XVI International Conference on High Energy Physics, Batavia, Illinois, September 6-13, 1972.)

Cross Sections

Photoproduction

There are four contributions to the Conference on vector meson photoproduction:

i. A final analysis of the laser experiment from the SLAC-Berkeley-Tufts collaboration,[3] presenting data on ρ, ω, Φ production at 2.8, 4.7 and 9.3 GeV;

ii. a DESY streamer chamber experiment from Aachen-Heidelberg-Munich[4] on ρ^o production with a tagged (4 - 6) GeV photon beam;

iii. a (2.0 - 4.7) GeV experiment on rho photoproduction from CEA, reported by Tannenbaum,[5] using a wire spark chamber setup;

iv. and finally, new data on rho production on hydrogen and deuterium, at energies between 9 GeV and 16 GeV, from a wire chamber experiment at SLAC.[6]

The new cross section data for rho photoproduction in the energy region (2 - 16) GeV is shown in Fig. 1, where the S-B-T[3] cross sections are derived assuming the Söding form for the mass and momentum transfer dependence of the dipion system, and where the SLAC-WSC[6] cross sections are obtained using the Söding model, but also integrating the form $\frac{d\sigma}{dt} = Ae^{-bt}$ with the parameters determined in the small momentum transfer region measured (i.e., $t < .3$ GeV^2).

Perhaps a more useful comparison is given in Fig. 2, where the new data on the forward rho cross section as a function of momentum is presented in Fig. 2a, and the updated world summary[7] is shown in Fig. 2b.

The CEA experiment[5] measured the differential cross section from $t \sim .2$ to $\sim .8$ GeV^2 in two energy regions — (2.9-3.7) GeV and (3.7-4.7) GeV. They report a slightly lower cross section with a greater slope than the S-B-T experiment.

The total reaction cross section, and the forward differential cross section both fall rapidly at low momentum, and remain fairly flat beyond (5 - 6) GeV. They exhibit a very similar energy dependence to πN scattering (viz $\sigma \propto p^{-0.2}$).

The ω photoproduction cross section is shown in Fig. 3 from threshold to 9 GeV. Again one sees a very rapid falloff of the cross section at low energies, flattening out around 5 GeV. The S-B-T laser experiment[3] is able to separate the cross section into the natural parity and unnatural parity contributions at 2.8, 4.7 and 9.3 GeV. The unnatural parity cross section falls very rapidly, in good agreement with the one-pion exchange model, and is essentially zero by 9 GeV. The natural parity exchange cross section, which one would hope to be diffraction dominated, falls off like the ρ photoproduction data discussed above (and hence like the πN data).

Finally, the ϕ photoproduction cross section is shown in Fig. 4. The new data to this Conference comes from the S-B-T laser experiment.[3] The energy dependence, beyond the initial rise from threshold, is either flat or rising very slowly. We will return to this point when discussing the ϕ differential cross section.

Hadron Data

Let us now look at data from hadron beams. In Fig. 5 the cross section for Q^o production† is shown as a function of momentum, from the SLAC $K^o_L p$ HBC experiment.[8] The $K^o_S \pi^+ \pi^- p$ reaction cross section rises rapidly from threshold, and then falls off as $p_{lab}^{-1.2}$. This is somewhat more rapid than the equivalent reactions for K^+p and K^-p, and is presumably due to the fact that the $K^\pm p$ reactions have substantial contributions from proton diffraction, $(p \to p\pi\pi)$, at the nucleon vertex, while such a process is forbidden in the K^o_L experiment due to the change of C at the $K^o_L \to K^o_S$ vertex. The cross section for Q^o production is quite flat from 5 GeV/c out to 12 GeV/c, having a momentum dependence of $p^{-.59 \pm .16}$.

---

†The Q refers to the low mass enhancement in the $K\pi\pi$ system, typically defined as the region between (1.0-1.5) GeV. It is usually associated with a $K^*\pi$ decay mode, and is thought to have $J^P = 1^+$.

Complimentary data on Q^+ production is shown in Fig. 6, from the world K^+ Collaboration.[9] The energy dependence from (2.5 - 12.7) GeV/c is studied as a function of the ($K\pi\pi$) mass, in 50 MeV steps from 1200 - 1500 MeV. All six mass intervals exhibit the same behavior, with an average momentum dependence of $p^{-0.60\pm0.05}$.

We also show, in Fig. 7, the energy dependence of the A_3 cross section† as determined by Ascoli et al.[10] This data comes from a large collaboration of bubble chamber groups with experiments from (5 - 25) GeV/c. The selection criteria for the A_3 events involves isolation of the $J^P = 2^-$, $f^o\pi$ amplitude in the 3π mass region (1.5 - 1.8) GeV. The energy dependence is quoted as $p^{-0.8\pm0.3}$.

The energy dependence of several diffractive processes are given in Table I, together with the comparable elastic scattering data. The inelastic diffractive processes all display quite similar energy dependence and fall off a little faster than the related elastic scattering reaction. However, they still have a rather flat energy dependence, and are quite different from a typical Regge exchange process which fall off, generally faster than $p^{-1.5}$.

Table I

Energy Dependence of Diffraction Process, $\sigma \propto p^{-n}$ ((5 - 20) GeV)

Process	n
$K^o \to Q^o$	0.59 ± 0.16
$K^+ \to Q^+$	0.60 ± 0.05
$\pi^- \to A_1^-$	0.41 ± 0.11
$N \to N\pi\pi$	0.4 ± 0.6
$\pi^- \to A_3^-$	0.8 ± 0.3

For comparison, the elastic scattering energy dependence is:

Process	n
K^+p	0.09 ± 0.03
K^-p	0.39 ± 0.04
πN	~ 0.2
NN	~ 0.2

Isospin Decomposition

The CERN-Brussels-Krakow HBC collaboration[11] have performed an isospin decomposition for the diffractive processes $K \to K\pi\pi$ and $N \to N\pi\pi$ at 5.0 and 8.2 GeV/c. The various charge states of ($K^*\pi$) and ($\Delta\pi$) were selected from the following reactions.

$$K^+p \to K^+\pi^-\pi^+p$$
$$K^+p \to K^o\pi^+\pi^op$$
$$K^+p \to K^o\pi^+\pi^+n$$

The event selection was made on the basis of mass cuts only with appropriate corrections being made for distortions to other distributions and for reflections of other reactions (e.g., the presence of $K^*\Delta$ double resonance production).

They find that the $K\pi\pi$ system is dominated by the I=1/2 amplitude, which is constant in magnitude between 5 and 8.2 GeV/c, as one would expect for a diffractive process. The mass distribution for the I=1/2 and I=3/2 amplitudes is shown in Fig. 8. The familiar Q enhancement is clearly seen in the I=1/2 data, and quite absent for the I=3/2 data.

It is interesting to note that the $N \to N\pi\pi$ process has appreciable I=3/2 contribution at these energies — (viz $\approx$ 30%).

Particle and Antiparticle Cross Sections

One interesting feature of the elastic scattering reaction is the near equality of the particle and antiparticle scattering cross sections at high energies (e.g., $\sigma(\pi^-p \to \pi^-p) \approx \sigma(\pi^+p \to \pi^+p)$. Let us examine this behavior for the diffractive dissociation process.

In Fig. 9 the ratio of the cross sections for $K^op \to Q^op$ and $\bar{K}^op \to \bar{Q}^op$ is shown as a function of momentum from (2 - 12) GeV/c.[8] The equal components of K^o and $\bar{K}^o$ in the K_L^o beam, for this experiment,

†The A_3 refers to the 3π enhancement in the (1500 - 1800) MeV region. It is usually associated with an $f^o\pi$ decay mode, and is thought to have $J^P = 2^-$.

allow a comparison of the cross sections to be made over the entire energy region free from problems of relative normalization between the strangeness states. The ratio is consistent with a constant value of $0.99 \pm .08$ over the entire energy region.

A similar comparison is shown in Fig. 10, where the cross section for pion dissociation ($\pi \to 3\pi$) and nucleon dissociation ($N \to N\pi\pi$) are compared for incident π^+ and π^- at 16 GeV/c, by the ABBCH collaboration.[12] The two dissociation reactions were isolated using Van Hove's LPS Analysis,[13] and the cross sections as a function of mass are shown in Fig. 10, with the ratio between π^+ and π^- initiated process displayed below. Again, the particle cross section is essentially equal to the antiparticle reaction cross section. More quantitatively,

$$R_{el} = \frac{\sigma(\pi^- p \to \pi^- p)}{\sigma(\pi^+ p \to \pi^+ p)} = 1.03 \pm 0.02$$

while

$$R_\pi = \frac{\sigma(\pi^- p \to (3\pi)^- p)}{\sigma(\pi^+ p \to (3\pi)^+ p)} = \begin{cases} 1.00 \pm 0.07 & \text{Ref. 12} \\ 0.94 \pm 0.12 & \text{Ref. 14} \end{cases}$$

and

$$R_N = \frac{\sigma(\pi^- p \to \pi^- (p\pi\pi))}{\sigma(\pi^+ p \to \pi^+ (p\pi\pi))} = \begin{cases} 0.97 \pm 0.07 & \text{Ref. 12} \\ 0.95 \pm 0.10 & \text{Ref. 14} \end{cases}$$

It appears that the inelastic diffractive processes exhibit the same property of equal particle and antiparticle cross sections, as found for elastic scattering processes.

Factorization Tests

If we really believed that these diffraction processes are dominated by the exchange of a simple Pomeron we should be able to factorize, or separate, the different vertices appearing in these processes.

For example, if we consider the processes illustrated in Fig. 11, with elastic pion and proton scattering at the upper vertex, and proton diffraction into a proton plus zero, one, two or three pions at the bottom vertex, the ratio between cross sections of the two upper vertex processes should be the same, independent of which of the four bottom vertices they interact.

$$\text{e.g.,} \quad R_1 = \frac{\sigma(\pi p \to \pi p)}{\sigma(pp \to pp)} \quad \text{should equal} \quad R_2 = \frac{\sigma(\pi p \to \pi(p\pi^0))}{2(pp \to p(p\pi^0))} \quad \text{etc.}$$

A paper has been submitted to the Conference by the Scandinavian Bubble Chamber Collaboration[15] in which the above diffractive processes have been isolated using the Van Hove Longitudinal Phase Space (LPS) analysis.[13] The results are given in Table II, and the agreement is surprising.

Another interesting test of factorization in diffractive processes was presented by the SLAC Streamer Chamber Group.[16] The reactions studied are given schematically in Fig. 12, where each of the diffractive contributions — $\gamma \to \rho^0$, $\pi \to \pi$ and $p \to p$ at the top vertex, and $p \to p$ and $p \to (p\pi\pi)$ at the bottom vertex — were isolated using the LPS analysis.[13] If the Pomeron contribution were well-behaved and factorizable, then we would expect the ratio of the cross sections for each of the top vertex process joined to both of the bottom vertex processes, to be equal. For example, we would expect $R_1 = R_2 = R_3$, where

$$R_1 = \frac{\sigma(\gamma p \to \rho^0 p)}{\sigma(\gamma p \to \rho^0 (p\pi\pi))}$$

Table II

Factorization Test in πN and pp Reactions

$R_1 = \frac{\sigma(\pi^- p \to \pi^- p)}{\sigma(pp \to pp)} = 0.43$
$R_2 = \frac{\sigma(\pi p \to \pi(p\pi^0))}{\sigma(pp \to p(p\pi))} = 0.46 \pm .15$
$R_3 = \frac{\sigma(\pi p \to \pi(p\pi^+\pi^-))}{\sigma(pp \to p(p\pi^+\pi^-))} = 0.35 \pm .18$
$R_4 = \frac{\sigma(\pi p \to \pi(p\pi\pi\pi))}{\sigma(pp \to p(p\pi\pi\pi))} = 0.45 \pm .15$

and

$$R_2 = \frac{\sigma(pp \to pp)}{\sigma(pp \to p(p\pi\pi))} \quad , \qquad R_3^{\pm} = \frac{\sigma(\pi^{\pm}p \to \pi^{\pm}p)}{\sigma(\pi^{\pm}p \to \pi^{\pm}(p\pi\pi))}$$

The experimental values for R_1, R_2, and R_3 are given in Table III for three different energy regions. Again the agreement is surprisingly good.

Table III

A Factorization Test for γp, πp, and pp Reactions

	Momentum (GeV/c)		
	(6 - 10)	(10 - 14)	(14 - 18)
$R_1 = \frac{\sigma(\gamma p \to \rho^0 p)}{\sigma(\gamma p \to \rho^0 p\pi^+\pi^-)}$	0.053 ± 0.014	0.035 ± 0.014	0.055 ± 0.024
$R_2 = \frac{\sigma(pp \to pp)}{\sigma(pp \to pp\pi^+\pi^-)}$	0.064 ± 0.007	0.061 ± .008	0.060 ± 0.009
$R_3^+ = \frac{\sigma(\pi^+p \to \pi^+p)}{\sigma(\pi^+p \to \pi^+p\pi^+\pi^-)}$		0.061 ± .006	0.063 ± 0.003
$R_3^- = \frac{\sigma(\pi^-p \to \pi^-p)}{\sigma(\pi^-p \to \pi^-p\pi^+\pi^-)}$		0.052 ± 0.005	0.059 ± 0.003

Some further tests of factorization were reported by the Scandinavian group[15] for processes in which diffraction dissociation occurs at both upper and lower vertex — the so-called double diffraction processes. Violation of the factorization prediction was observed in these reactions.

In summary, the cross section data for diffraction dissociation processes behave very much like the corresponding elastic scattering data. It will be of interest to now study the differential cross sections to see if the same regularities appear there.

Differential Cross Sections

Vector Meson Photoproduction

The differential cross section for rho photoproduction at 9.3 GeV,[3] and at several energies between 9 and 16 GeV[6] are shown in Fig. 13a and 13b respectively, as examples of the new data presented to this Conference. The data from both experiments have been analyzed using the Söding model for the mass and momentum transfer dependence of the dipion system. The slopes of the differential cross section, assuming an exponential form, are shown in Fig. 14 for the new data, and again for all available data,[7] (analyzed using the Söding model) in Fig. 15. There is a slight suggestion of shrinkage for rho photoproduction for energies between (3 - 16) GeV of about (1 - 1½) units. However, considering the systematics involved in fitting the rho mass shape and the different t regions studied in the experiments, it would be hard to press such a conclusion.

The constancy (or at least small energy dependence), of the slope in the rho differential cross section is reminiscent of the situation in πN elastic scattering. Earlier in this session, Harari[17] discussed the Dual Absorptive Model, and its recent successful application to πN scattering, by Davier.[18] An extension of this work to rho photoproduction by Chadwick et al.[19] has been presented to the Conference. They assume that Pomeron and peripheral f^0 dominate the exchange process and a Regge behavior for the f^0 amplitude, and hence uncover shrinkage in the Pomeron contribution to $\gamma p \to \rho^0 p$ which behaves just like the shrinkage in

K^+p elastic scattering at these energies, and also agrees well with Davier's analysis. Their fits to the data, and results for the Pomeron and f^0 slopes as a function of energy are shown in Fig. 16.

The ω differential cross sections from the S-B-T collaboration[3] are given in Fig. 17. The slope of the cross section is found to be ~ 7 GeV^{-2} and quite independent of energy. (An analysis of the natural parity contribution results in the same conclusion, but with somewhat larger errors.) The CEA experiment[5] reports good agreement with the above data.

The situation for ϕ photoproduction is rather more complicated. The differential cross sections presented to this Conference are shown in Fig. 18. The S-B-T HBC collaboration[5] present their data at 2.8, 4.7 and 9.3 GeV, while Anderson et al.,[20] present 12 GeV data from the SLAC 1.6 GeV spectrometer. The slopes of these differential cross sections are shown in Fig. 19, together with earlier work. They also appear in Fig. 16 for comparison with the Pomeron contribution to the rho reaction. Given the accuracy of the data and the different momentum transfer regions of the several experiments shown in Fig. 18, one could easily accomodate some shrinkage (as indicated in Fig. 16), but equally justified would be the conclusion of a flat energy dependence.

The Ritson group[20] have also measured the energy dependence of ϕ photoproduction for a given momentum transfer, namely $t=0.6$ GeV^2. Their results are shown in Fig. 20, and clearly indicate that there is no shrinkage at this value of t. In fact, an analysis in terms of $\alpha=\alpha(0)+\alpha' t$ yields $\alpha'=(-0.03\pm 0.13)$. This flat, or energy independent, differential cross section is not what was expected from our naive understanding of diffractive processes.

Why do we care so much about the ϕ photoproduction data, and become disturbed when the data do not uphold our prejudices? The reason is that the process $\gamma p \to \phi p$ is supposed to be one of the clearest ways to study the Pomeron. The ϕ meson does not couple to non-strange hadrons, and therefore the only contribution expected to the t-channel exchange is from the Pomeron. We would therefore hope to learn in an unambiguous way about the details of the Pomeron amplitude.

If the ϕ photoproduction is pure Pomeron exchange, why is the behavior of the differential cross section so different from $K^+p \to K^+p$, which we believe to be mainly Pomeron exchange, or even from the Pomeron behavior derived from Davier's[18] analysis of πN scattering and the Chadwick et al.[19] analysis of rho photoproduction and Compton scattering?

Many questions arise at this point. Does the ϕ cross section increase (see Fig. 4), and if so does it increase fast enough that the ϕ slope could be increasing like the K^+p slope, but with the cross section at $t=.6$ GeV^2 staying roughly constant? (The answer to this question is no; the cross section does not increase fast enough to allow the forward slope to increase at the canonical "K^+p Pomeron" rate.) What are the possible relationships between the small values of α' found at ISR energies for p-p scattering and the Ritson result for $\gamma \to \phi$? Could ϕ photoproduction exhibit shrinkage for smaller t regions, as found in ISR p-p scattering? I do not wish to follow up these questions here. The situation to be addressed is that $\gamma p \to \phi p$ is different from $K^+p \to K^+p$ and $pp \to pp$ at the same energies, at least for $t \sim 0.6$ GeV^2.

We do have experimental information supporting the hypothesis that the $\gamma p \to \phi p$ reaction is diffractive. The SLAC spectrometer experiment of Anderson et al.,[21] measured the asymmetry parameter $\Sigma=\sigma_{\parallel}-\sigma_{\perp}/\sigma_{\parallel}+\sigma_{\perp}$, for the photoproduction of ϕ mesons with photons polarized parallel and perpendicular to the plane of decay. The experiment was performed using a diamond crystal to polarize the photon beam, and detecting the ϕ production via the recoil proton and the ϕ decay by detecting the K^+K^- pairs in a forward spectrometer. They found $\Sigma=0.985\pm 0.12$ for a photon energy of 8.1 GeV, and for momentum transfer, $t=0.2$ GeV^2. This is consistent with pure natural parity exchange. This conclusion is supported by the S-B-T laser experiment[3] study of ϕ photoproduction, where the asymmetry and density matrix elements at 4.7 and 9.3 GeV are also consistent with pure natural parity exchange. Further support comes from the DESY/MIT group[22] who report observation of strong coherent production of ϕ mesons from carbon at 5.2 GeV.

However, there is one piece of evidence that although the forward $\gamma \rightarrow \phi$ process may be dominantly natural parity exchange, it is not purely imaginary as would be expected for Pomeron exchange. The DESY/MIT group[23] have measured the interference between the resonant ϕ production amplitude and the Bethe-Heitler amplitude in $\gamma C \rightarrow Ce^+e^-$ for photon energies around 7 GeV. They report that the ϕ amplitude differs from being purely imaginary by $25^o \pm 15^o$, or rather, that Re A_ϕ/Im $A_\phi = -0.48^{+0.33}_{-0.45}$. This may be an indication that the $\gamma \rightarrow \phi$ process is not purely due to Pomeron exchange, but unfortunately the accuracy obtainable in this difficult experiment does not allow any firm conclusions to be drawn.

We clearly have insufficient data to make definitive statements on the energy dependence of the ϕ cross section for momentum transfers other than 0.6 GeV^2. As the shrinkage, or nonshrinkage, of this cross section is of special interest for studies of the Pomeron it is highly desirable to have another energy sweep, similar to Anderson et al.[21] but for a t value around 0.2 GeV^2, or even smaller.

Hadron Dissociation

The differential cross section for A_1 production at 40 GeV/c is shown in Fig. 21, from the CERN-IHEP collaboration.[24] The data fit an exponential over the small region of t studied, and the slope is given as ~ 7 GeV^{-2} for the three pion mass region (1.215 - 1.415) GeV. This cross section shows remarkable stability from 16 GeV/c to 40 GeV/c; the slopes for two (3π) mass regions, in the reaction $\pi^- p \rightarrow (\pi^+\pi^-\pi^-)p$ are given in Table IV.

Table IV

Mass (3π) (GeV)	16 GeV/c (ABBCCH Collab[12])	40 GeV/c (Antipov et al.[24])
(1.0 -1.2)	(10.6 ±0.9) GeV^{-2}	(11.2 ±0.9) GeV^{-2}
(1.25-1.45)	(7.1 ±0.5) GeV^{-2}	(6.7 ±0.9) GeV^{-2}
	(0.02<t<0.4 GeV^2)	(0.04<t<0.33 GeV^2)

Data was also presented on the A_3 cross section by the Ascoli et al. collaboration.[10] The cross section, averaged over the momentum interval (11 - 25) GeV/c, for the $f^o\pi$, $J^P=2^-$ amplitude in the mass region (1.5 - 1.8) GeV is shown in Fig. 22. The slope is (7.7 ± 0.8) GeV^{-2}

A summary of the slopes of various diffraction cross sections is shown in Table V, and the corresponding elastic data is listed for comparison. It is interesting to note that the diffraction processes exhibit the same kind of regularities with respect to each other as found for the corresponding elastic data, and further that the absolute value of the slopes for diffraction reactions is about the same as for elastic scattering, always being a little ($\sim$ 1 - 2 units) higher.

Table V

Process		Slope (GeV^{-2})
$\gamma \rightarrow \rho$	~	6-8
$\pi \rightarrow A_1$	~	9-11
$\pi \rightarrow A_3$	~	8
$K \rightarrow Q$	~	5-7
$\bar{K} \rightarrow \bar{Q}$	~	8-10
$N \rightarrow (N\pi\pi)_{1400}$	~	10-11
$N \rightarrow (N\pi\pi)_{1700}$	~	5

For comparison, the elastic slopes are ~

Process		Slope (GeV^{-2})
γN	~	6
πN	~	7-9
KN	~	5-6
$\bar{K}N$	~	7-8
NN	~	9-10

The Cross-Over Phenomenon

The differential cross section for the elastic scattering reaction $\bar{X}p \rightarrow \bar{X}p$ (where X is π^+, K^+, p) is known to have a steeper slope and a larger forward intercept than the reaction $Xp \rightarrow Xp$. This leads to the well-known "cross-over" phenomenon[25] in which these two elastic reactions have the same differential cross section, $\frac{d\sigma}{dt}$, for t $\sim$0.2 GeV^2. This effect has recently been discussed within the framework of the Dual Absorption Model by Davier and Harari.[17] Basically the elastic scattering is described by a dominant Pomeron exchange amplitude, but also has contributions from Regge amplitudes. The K^+p and pp scattering are exotic in the s-channel and so, from duality arguments, have

contributions only from Pomeron exchange, whereas $\pi^{\pm}p$, $K^{-}p$, and $\bar{p}p$ all have a mixture of Pomeron and Regge contributions. Some preliminary data from Diebold et al.,[26] at Argonne, Fig. 23, show the cross-over effect at 6 GeV for all three sets of particle and antiparticle elastic scattering. The Kp and pp data show a very clear cross-over while the $\pi^{\pm}p$ cross sections have very similar slope and magnitude. Naively, this can be understood as the result of both Regge and Pomeron contributions to $\pi^{+}p$ and $\pi^{-}p$, while for other processes the Regge contribution only arises for the antiparticle scattering. The interference effects between the Pomeron and odd C exchanges cancel when one integrates over the total cross section, thus yielding the equal particle and antiparticle cross sections discussed above.

We have observed that the diffraction processes have many of the same properties as the elastic scattering reaction, and it is therefore interesting to study the differential cross section for particle, antiparticle reactions for evidence of this cross-over phenomena.

Several papers have been presented to this Conference reporting evidence for the observation of cross-overs in the differential cross section for inelastic diffractive processes. The SLAC $K^{o}_{L}p$ HBC report on the study of the reactions $K^{o}p \to Q^{o}p$ and $\bar{K}^{o}p \to \bar{Q}^{o}p$, in the momentum region from (4 - 12) GeV/c.[8] The relative normalization of the K^{o} and $\bar{K}^{o}$ differential cross sections are taken care of automatically through the natural composition of the K^{o}_{L} beam. The cross sections are shown in Fig. 24, where we see that the $\bar{Q}^{o}$ data has a larger forward cross section and a steeper slope, giving rise to a cross-over of the two differential cross sections at $t = (0.13 \pm .03)$ GeV^2. The slopes of the differential cross sections for the momentum transfer region ($0.02 < t' < 0.5$ GeV^2) and averaged over (4 - 12) GeV/c are $b(Q^{o}) = (5.9 \pm 0.5)$ GeV^{-2} and $b(\bar{Q}^{o}) = (9.7 \pm 0.5)$ GeV^{-2}. This is in good agreement with $K^{\pm}p$ elastic scattering, where a cross-over is observed for $t \sim 0.20$ GeV^2 and where the slopes are ~ 5.5 GeV^{-2} for $K^{+}p$ and ~ 7.5 GeV^{-2} for $K^{-}p$ in the (5 - 10) GeV/c region.[27] It is also in good agreement with preliminary SLAC data on $K^{\pm}p$ elastic scattering at 13 GeV/c[28] presented to this Conference and shown in Fig. 25. They report a $K^{+}p$ slope of 5.52 ± 0.05 GeV^{-2}, and a $K^{-}p$ slope of 7.15 ± 0.06 GeV^{-2}.

This effect should also be present for $K^{\pm}p \to Q^{\pm}p$, but the relative normalization of different experiments which involve different detectors and analysis techniques is very difficult and makes a detailed comparison almost impossible. However, the difference in slopes of the cross sections can be observed. Below are several examples taken from the literature, in which one sees the same effect reported above by the SLAC $K^{o}_{L}p$ experiment (viz the $Q^{-}p$ slope is observed to be greater than the $Q^{+}p$ slope).

Similar investigations have been reported for A_1 production in $\pi^{\pm}p \to A_1^{\pm}p$; a HBC experiment at 16 GeV/c from the ABBCH collaboration[12] and a wire spark chamber experiment from SLAC[33] at 15 GeV/c. The cross sections are shown in Fig. 26 and Fig. 27 respectively. From the data in Fig. 26 the cross sections are reported to cross over at $t \sim 0.15$ GeV^2. The difference in slopes for the A_1^{-} and A_1^{+} (defined as $0.95 \leq M(3\pi) \leq 1.25$ GeV), are found to be

Table VI

Momentum (GeV/c)	$K^{-}p \to Q^{-}p$ Slope (GeV^{-2})	$K^{+} \to Q^{+}p$ Slope (GeV^{-2})
10	8.5 ± 1.0 Ref. 29	6.7 ± 0.5 Ref. 31
12	11.0 ± 2.0 Ref. 30	7.4 ± 0.3 Ref. 32

$$b(A_1^{-}) - b(A_1^{+}) = \begin{cases} (2.0 \pm 0.9) \text{ GeV}^{-2} & \text{Ref. 12} \\ (1.1 \pm 0.8) \text{ GeV}^{-2} & \text{Ref. 33} \end{cases}$$

For comparison, the difference in slopes for πN elastic scattering at this energy is:

$$b(\pi^{-}p) - b(\pi^{+}p) = (1.5 \pm 0.8) \text{ GeV}^{-2} \qquad \text{Ref. 34}$$

(It is very interesting to note that the high energy πN elastic scattering slopes are no better known than the cross sections for the A_1 process!)

The ABBCH experiment also compared the cross sections for the process where the proton diffracts into a $(p\pi\pi)$ system (i.e., $\pi^{\pm}p \to \pi^{\pm}(p\pi^{+}\pi^{-})$). They find the difference in slopes to be $b(\pi^{-})-b(\pi^{+}) = (0.0\pm1.7)$ GeV^{-2}. (Quite compatible with πN elastic scattering data.)

Thus, the diffraction dissociation process appears to exhibit a similar cross-over phenomena — both in position and in magnitude — to that observed in elastic scattering processes.

Mass Dependence of Differential Cross Sections

Let me briefly comment on the dependence of the slope of the differential cross section on the mass of the produced system.

In Fig. 28 the slope of the differential cross section for $\gamma p \to \pi^{+}\pi^{-}p$ is shown as a function of the dipion mass. The data is from the S-B-T laser experiment.[3] The solid curve is the prediction of the Drell-Söding model which proposes a coherent one-pion exchange contribution under the rho. The interference between the rho amplitude and this Söding term causes the observed skewing of the π-π mass spectrum in photoproduction, produces quite characteristic effects in the decay distribution of the rho and leads to the rapid change in the differential cross section seen in Fig. 28.

The same effect is seen in other hadron dissociation processes. Examples are given in Fig. 29 for $Kp \to Qp$ and in Table VII for $\pi N \to A_1 N$ and $\pi N \to \pi N^{*}$. It is a well-known effect, and finds an explanation in

Table VII

Cross section $(d\sigma/dt')_{t'=0}$ and slope parameter A, for the reactions $\pi^{\pm}p \to (\pi^{\pm}\pi^{+}\pi^{-})p$ and $\pi^{\pm}p \to \pi^{\pm}(p\pi^{+}\pi^{-})$ at 16 GeV/c, as a function of (3π), and $(p\pi\pi)$ mass.

Mass, GeV	$\pi^{-}p \to (\pi_f^{-}\pi_s^{-}\pi^{+})p$		$\pi^{+}p \to (\pi_f^{+}\pi^{-}\pi_s^{+})p$	
	$\left(\frac{d\sigma}{dt'}\right)_0 \cdot \frac{mb}{GeV^2}$	A, GeV^{-2}	$\left(\frac{d\sigma}{dt'}\right)_0 \cdot \frac{mb}{GeV^2}$	A, GeV^{-2}
All	4.9 ±0.4	9.1±0.3	3.7 ±0.3	7.2±0.3
0.6 - 1.0	1.0 ±0.1	14.6±1.8	0.58±0.05	11.3±0.5
1.0 - 1.12	1.2 ±0.1	11.5±0.8	0.8 ±0.1	9.6±0.7
1.12 - 1.28	1.2 ±0.1	9.8±0.7	1.0 ±0.1	7.6±0.6
1.28 - 1.40	0.57±0.06	7.1±0.5	0.40±0.06	5.0±0.6
1.40 - 3.00	1.3 ±0.2	7.2±0.7	1.0 ±0.1	5.7±0.3

Mass, GeV	$\pi^{-}p \to \pi_f^{-}(\pi_s^{-}\pi^{+}p)$		$\pi^{+}p \to \pi_f^{+}(\pi_s^{+}\pi^{-}p)$	
	$\left(\frac{d\sigma}{dt'}\right)_0 \cdot \frac{mb}{GeV^2}$	A, GeV^{-2}	$\left(\frac{d\sigma}{dt'}\right)_0 \cdot \frac{mb}{GeV^2}$	A, GeV^{-2}
All	1.4 ±0.2	5.9±0.4	1.6 ±0.2	6.5±0.4
1.2 - 1.52	0.63±0.08	11.7±1.2	0.65±0.08	11.8±1.2
1.52 - 1.64	0.26±0.03	7.5±0.6	0.35±0.05	8.3±0.9
1.64 - 1.80	0.30±0.03	4.7±0.3	0.29±0.04	4.6±0.7
1.80 - 2.08	0.17±0.03	2.5±0.9	0.26±0.04	5.3±0.8
2.08 - 3.20	0.18±0.03	4.0±0.8	0.17±0.03	3.7±0.7

a generalization of the Drell-Söding model discussed above, and called the Reggeized Deck Model. In this model the A_1 and Q diffraction processes, for example, are described by the diagrams labeled (a).

This model does a fair job of describing the observed mass spectra, the cross section as a function of energy and the change of slope as a function of mass. However, it cannot be the whole story. Consider the $K_L^o p$ data discussed above in connection with the cross-over effect. These reactions would be pictured as shown by the diagrams labeled (b).

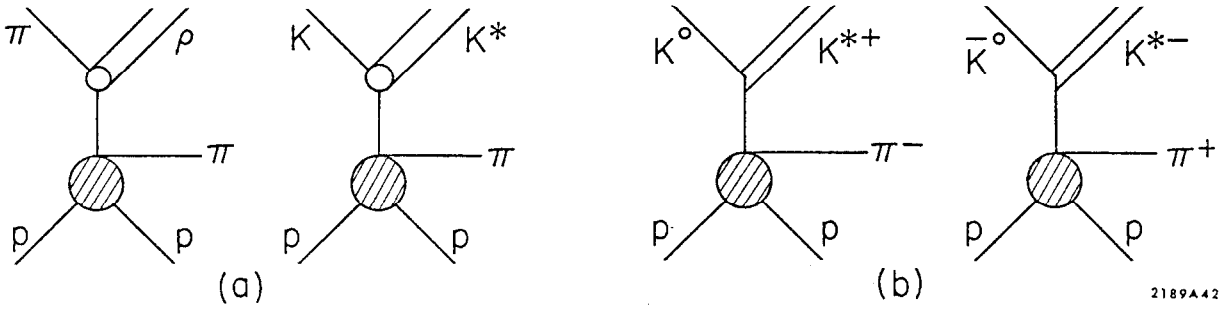

Since $\pi^- p$ elastic scattering has a steeper slope than $\pi^+ p$ elastic scattering, this description would predict that $K^o \to Q^o$ would have a steeper differential cross section than $\bar{K}^o \to \bar{Q}^o$ in contradiction to the data.

Although the RDM clearly does quite a fair job in describing these diffractive processes, it cannot be the whole story and contributions from the vector exchanges, at the very least, must be included.

Spin Structure

Let me remind you that early work by the S-B-T collaboration[3] on polarized photoproduction of rho mesons, showed that s-channel helicity conservation (SCHC) was observed in this process for momentum transfers less than 0.4 GeV^2. These studies led Gilman and co-workers[35a] to suggest that SCHC may be a general property of all Pomeron exchange processes. This is further supported by new measurements on the A and R parameters for elastic p-p scattering at 6 and 16 GeV/c, presented to this Conference.[35b] Recent work on πN scattering[36] has shown that SCHC is not an exact property of πN elastic scattering, but that ~15% of helicity-flip amplitude must be present at momenta ~6 GeV/c for the t range (0.2 - 0.6) GeV^2. It is therefore, in principle, of interest to determine the helicity structure of the diffraction process, and then further compare them to the elastic reactions.

However, there are severe problems in such a program. Many questions arise: what is the signal we are studying — is the diffracting system a single particle? Can we consider the diffracting system a single system? If we have a resonance plus coherent background situation, what is their relative phase and how would it affect the helicity conservation analysis? Despite these basic difficulties many people have been working on the question. I have tried to summarize this work and their conclusions in Table VIII.

One fairly clear situation has been studied in depth — rho photoproduction. Here the coherent background amplitude is fairly well understood and ~10% of the resonant signal. The S-B-T collaboration[19,37] have shown evidence for possible helicity flip in $\gamma p \to \rho^o p$. There are difficulties, as mentioned above — mainly with regard to the relative phase between the rho and Söding amplitudes — but taken at face value they find a helicity flip contribution to the meson vertex, in $\gamma \to \rho$, of the same magnitude as found for the nucleon vertex in the πN scattering case (i.e., ~15% of the SCHC amplitude) at the same energy. The SCHC violation is observed to be in the natural parity exchange amplitude. This, taken together with the fact that the magnitude of the effect is consistent with being independent of energy, implies that the small s-channel helicity violation is a property of the Pomeron.

Table VIII

Reaction	p_{lab} (GeV/c)	Group	Paper	Analyzer	SCHC	TCHC
$\gamma \to \rho^0$	2.8, 4.7, 9.3	Ballam et al.	307, 411	Azimuthal and polar angle of π.	Yes (They report a possible 2% flip contribution.)	No
	(2.7 - 4.0)	Gladding et al.	206	Same	Yes ($t < .5$ GeV)	No
	(4 - 6)	Struczinski et al.	325	Same	Yes	No
	(9 - 16)	Bulos et al.	349	Same	Yes	No
$\gamma \to \omega$	2.8, 4.7, 7.3	Ballam et al.	411	Same	Yes	No
$\gamma \to \phi$	2.8, 4.7, 7.3	Ballam et al.	411	Same	Consistent	No
$\pi \to A_1$ ±	8.16	ABBCH	390	LPS selection, and polar angle of π.	No	No
$\pi \to A_1$ ±	16	ABBCCHLVW	169	Azimuthal study, normal to 3π and polar angle of π.	No	No
$\pi \to A_1$ -	40	Antipov et al.	442		No	Slight Violation
$\pi \to A_1$ -	4.5	Beketov et al.	833	Normal to 3π plane.	No	Yes
$\pi^- \to A_3^-$	(5 - 2.5)	Ascoli et al.	341	π^+ polar angle	No	Yes (but not very strong)
$K \to Q$ -	10	ABBCCHLVW	169	Azimuthal study, and normal to plane and π polar angles.	No	No
$K \to Q$ -	14.3	Barloutaud et al.	371	Normal to $K\pi\pi$ plane, and polar angles of π.	No	No
$K \to Q$ 0	(4 - 12)	Brandenburg et al	347	Normal to $K\pi\pi$ plane.	No	Yes (but not very strong)
$p \to p\pi\pi$ 1400	10, 16	ABBCCHLVW	169	Azimuthal study, and normal, and polar.	Data Insensitive	
$p \to p\pi\pi$ 1700	10, 16	ABBCCHLVW	169	Same	No	Yes
$p \to p\pi\pi$ All	8, 16	ABBCH	390	LPS and polar angles of π.	No	Yes
$p \to p\pi\pi$ All	25	Chapman et al.	452	Azimuthal	No	No
$p \to p\pi\pi$ 1600	11.6	Oh et al.	260		No	Yes

In summary, the vector meson photoproduction process is mainly (~ 90% of the amplitude) s-channel helicity conserving and behaves very much like πN scattering. The hadron dissociation processes $(\pi \to 3\pi)$, $(K \to K\pi\pi)$, $(N \to N\pi\pi)$, do not conserve s-channel helicity and although they approach t-channel helicity conservation, they do not rigorously conserve that either. Finally, at this point, until we understand more of what is going on in diffraction dissociation, we will not profit by more investigations of the spin structure of these various mass regions.

Mysteries and Nasty Questions

In this section we review briefly some bogey-men for our "conventional diffraction" world.

Michigan-Princeton Neutron Dissociation Experiment

A wire spark chamber experiment studying the diffraction dissociation of high energy neutrons on nuclear targets at BNL has been reported to the Conference.[38] The reactions observed were:

$$nA \to p\pi^- A \quad , \qquad \text{where} \quad A = C,\ Cu,\ Pb$$

and where the neutron beam had a momentum spectrum stretching from (18 - 29) GeV/c, with a mean effective momentum of ~ 23 GeV/c.

The production angular distribution of the $(p\pi^-)$ system is shown in Fig. 30, for the carbon and copper targets. Sharp forward peaks, with slopes characteristic of the carbon and copper nuclear radius, are observed indicative of coherent production. In Fig. 31, the effective mass distribution of the $(p\pi^-)$ system is shown for events in the coherent peak (the incoherent background is estimated at $\lesssim$ 30% for this forward t region). An estimate of the mass acceptance of the spectrometer is sketched in under the carbon mass distribution in Fig. 31, and is shown to be quite large and smoothly varying over the mass region of interest. The mass resolution of the system is reported as ± 10 MeV at a $p\pi^-$ mass of 1200 MeV, derived from actual measurements of e^+e^- pairs produced in a lead target by the small contamination of photons in the neutral beam.

The surprising result of this experiment is the lack of any structure in the mass plots. (On lead, there is evidence of Coulomb production of the Δ(1236), but that phenomena is outside the scope of this talk.) The N*(1470) and N*(1688) which one would have expected to be copiously produced are just not present — an upper limit of 6% and 5% respectively, of the total $p\pi^-$ cross section is estimated by the authors.

Even more surprising are the conclusions from a study of the decay angular distribution of the $p\pi^-$ system. In Fig. 32 the polar angular distribution of the π^- in the $p\pi^-$ rest frame are given for both Jackson and Helicity frame coordinate systems. The data is displayed for four momentum transfer regions the first of which is dominantly coherent, the second having about equal contributions from coherent and incoherent processes and the other two being dominated by incoherent processes. The distributions are presented for, $-0.04 < \cos\theta_\pi < 1.0$, the region in $\cos\theta_\pi$ for which the detection efficiency is reasonably well understood. The small t, coherent region shows a very sharp forward peak, where the π^- goes forward in the $p\pi^-$ rest frame.

For a process in which the neutron dissociated into a $p\pi^-$ system with the same quantum numbers as the neutron, we would expect (at t=0) a flat decay distribution in Fig. 32a. The solid curve, which fits the data rather well, is a $(1+3\cos^2\theta)$ distribution, characteristic of J=3/2 rather than the J=1/2 expected from simple dissociation. In fact, the authors point out that this distribution does not demand that the $p\pi^-$ system be in a pure J=3/2 state, but that a mixture of S-, $p_{1/2}$ and $p_{3/2}$ waves could give rise to the observed decay distribution. However, the main point of their study is that a substantial J=3/2 amplitude is present in this low mass $p\pi^-$ diffraction dissociation system. The $p\pi^-$ mass region used for Fig. 32 was (1100-1320) MeV, but the higher mass region gives similar results.

This experiment confronts us with several real puzzles. Why are there no signs of the N^*_{1470} and N^*_{1688} resonances in the neutron dissociation, but only the broad low mass enhancement reminiscent of the (3π) and $(K\pi\pi)$ final states in πp and Kp collisions; and why does the neutron dissociation process favor the $\Delta J=1$ spin change (again like the π and K dissociations) instead of coupling to the $J^P=\frac{1}{2}^+$ states? Somehow one expected the $n \to p\pi^-$ reaction to be more reminiscent of $\gamma \to \rho$ than the other murkier processes $(\pi \to 3\pi)$, $(K \to K\pi\pi)$, but that seems to have been too naive a hope.

A similar investigation has been reported to the Conference by Oh et al.,[39] where they study the reaction $\pi^- n \to \pi^-\pi^- p$ at 11.7 GeV/c in a deuterium bubble chamber. The same low mass enhancement for the $p\pi^-$ system is observed for the small momentum transfer region — see Fig. 33 — with little or no sign of structure. However, they report quite different decay angular distributions than the Michigan-Princeton experiment discussed above — see Fig. 34. The higher mass regions around 1500 MeV and 1700 MeV appear to be dominated by $3/2^-$ and $5/2^+$ waves, implying production of the D13 and F15 resonances following the natural spin-parity sequence expected in diffractive processes. The relative phase between the D13 and F15 is found to be zero, again in agreement with a diffractive N* production picture.

However, the question remains, what about the discrepancy between these two experiments for the $(p\pi^-)$ decay distribution in the mass region up through 1500 MeV. It is highly desirable to have a repeat of the high statistics Michigan-Princeton experiment, but with a complete decay angular acceptance, to shed further light on this interesting problem.

The A_2 Question

There have been suggestions for some time that perhaps the A_2 meson is produced via Pomeron exchange, thus violating our simple rule of natural spin-parity excitation in diffraction processes. Kruse et al.[41] have submitted an analysis of A_2 production in bubble chamber data in the energy range from (5 - 25) GeV/c. There is also a paper from Ascoli et al.[42] on A_1, A_2 and A_3 production at 40 GeV/c. The facts are summarized below:

i. The A_2 cross section falls off as $p^{-0.8\pm0.08}$ in the (5 - 25) GeV/c range;
ii. the relative energy dependence of A_1, A_2 and A_3 between 25 GeV/c and 40 GeV/c are essentially the same;
iii. the natural parity exchange contribution to A_2 production falls off as $p^{-0.57\pm0.09}$
iv. the t-channel exchange in A_2 production is mainly isoscalar;
v. the s-dependence of the cross section implies an effective intercept, $\alpha_{eff}(0) \sim 0.7$;
vi. an analysis of the shrinkage of the $J^P=2^+$ A_2 differential cross section yield an $\alpha_{eff}(0) \sim 0.8$.

The energy dependence and α_{eff} values quoted above are more in agreement with a strong Pomeron contribution to A_2 production than the vector, and tensor meson contributions one expected. However, we must understand at least one other fact before throwing away our current picture of Pomeron processes — the energy dependence for the A_2 cross section as measured in the $K\bar{K}$ decay mode seems to be faster than $p_{lab}^{-1.0}$. This is a clean reaction in which to study A_2 production with very little background, and the observed momentum dependence is very much in agreement with that expected for meson exchange in the t-channel. Several experiments should be reporting new cross sections for $A_2 \to K\bar{K}$ within the near future, and we wait impatiently for their results.

G-Parity Conservation

While discussing various possibilities of the Pomeron not conforming to our prejudices, I thought it would be comforting to quote the results of a paper by Arnold et al.,[43] on 11.7 GeV/c π^- interactions in a heavy liquid bubble chamber. They observe strong coherent A_1 production with a cross section of

~ 2 mb/nucleon, while there is no evidence of B-meson production with an upper limit of < 30 μb/nucleon. At least the Pomeron does respect G-parity conservation!

$K^- p \to K^{*-} p$

A year ago at the Oxford Conference Barloutaud,[44] in revieving two-body processes, reported that the $K^- p \to K^{*-} p$ cross section stopped falling like p_{lab}^{-2} around 8 GeV/c and appeared to flatten out to an energy independent cross section. Immediately the cry went up that Pomeron exchange may be important in this reaction and that our ideas of the spin-parity series involved in Pomeron couplings would have to be thrown away. New data to this Conference on 16 GeV/c $K^- p$ interactions, reviewed in another talk by Goldschmidt-Clermont[45] showed that this particular challenge has gone away. The K* cross sections continue to fall through 16 GeV/c, and all the data are in good agreement with isoscalar natural parity exchange — presumably ω exchange.[46]

One interesting contribution on this topic by Bingham et al.,[47] reported the observation of coherent K^{*-} production in a heavy liquid bubble chamber experiment at K^- momenta of 5.5, 10.0 and 12.7 GeV/c. The (Kπ) mass distribution and the K^*_{890} momentum transfer distribution are shown in Fig. 35. The K^*_{890} cross sections observed were in good agreement with the coherent amplification of the K* cross sections reported on hydrogen.

The threat of Pomeron exchange being responsible for the $K^- \to K^{*-}$ process seems to have disappeared and everything is in good agreement with ω exchange.

Photoproduction of the B-Meson

Finally, in this section on "bogey-men", we deal with the photoproduction of the B-meson. The reaction $\gamma p \to Bp$ violates the natural spin-parity series expected in diffractive processes, yet the B signal is observed with the same strength at 2.8, 4.7 and 9.3 GeV.[48] The energy independent cross section has encouraged speculation as to the validity of the simple rules on spin couplings for the Pomeron.

However, the statistics on these observations are rather limited, each energy point having a cross section of (1.0 ± 0.4) μb. One could accommodate quite a variety of energy dependences within these measurements. It is an important reaction and to be followed with interest — but the present results are not strong enough to call our ideas on Pomeron coupling to question — at least not yet.

Conclusion

The experimental situation for vector meson photoproduction seems to be fairly complete and consistent. The cross section, differential cross section and spin structure seem to be very similar to elastic πN scattering (for the ρ^0 and ω), even down to the few percent s-channel helicity violating cross section. φ photoproduction perhaps presents an exception to this rosy picture, but more data on the energy dependence of the small t cross section is required before problems can be precisely defined. It will be interesting to see vector meson photoproduction data from NAL in the future.

The situation for the hadron dissociation is not so clear. The diffraction dissociation final states do appear to have a well defined spin parity, and so one can identify and discuss the reactions with some meaning. However, it is surprising that no mass structure, or even resonance behavior of the phases is observed, even in situations where resonances exist which do couple to the final state being studied.

A major question remains to be answered: What is the dynamics in diffraction processes? Certainly a large part of the story must be due to kinematics, but a small resonance contribution is not completely excluded. But why is it so small? Does the Pomeron have strange properties when coupling to inelastic final states?

Despite all of the above questions, we have seen an encouraging degree of regularity emerging in the diffraction dissociation data, and many similarities to the elastic scattering behavior: the flat energy dependence of the cross section; the equality of particle and antiparticle cross sections; the factorizability of diffractive vertices; the sharp forward peak in the differential cross section and the observation of

cross-over in the differential cross section for particle and antiparticle scattering. The spin structure is, however, quite different for the diffraction dissociation process, being neither s- nor t-channel helicity conserving.

Acknowledgements

I would like to thank Prof. F. Gilman and Dr. R. Cashmore for reading the manuscript, and for their helpful comments.

References

1. G. Kane, "Phenomenology of diffractive reactions," Rutherford Preprint RPP/T/20.
2. H. Lubatti, "Diffraction dissociation of hadrons," Washington University Preprint, VTL PUB 9.
3. J. Ballam et al. (SLAC-Berkeley-Tufts Collaboration), Paper No. 411, contribution to this Conference
4. W. Struczinski et al. (Aachen-Heidelberg-Munich Collaboration), Paper No. 325, contribution to this Conference.
5. G. Gladding et al., Paper No. 206, contribution to this Conference.
6. F. Bulos et al., Paper No. 349, contribution to this Conference.
7. G. Wolf, Rapporteur's talk at Cornell Conference on Electron and Photon Physics.
8. G. Brandenburg et al., Paper No. 347, contribution to this Conference and SLAC-PUB-1038.
9. H. H. Bingham et al. (International K^+ Collaboration), Paper No. 218, contribution to this Conference.
10. G. Ascoli et al. (A_3 Collaboration), Paper No. 341, contribution to this Conference.
11. Brussels-CERN-Krakow Collaboration, Paper No. 557, contribution to this Conference.
12. ABBCH Collaboration, Paper No. 389, contribution to this Conference.
13. W. Kittel, S. Ratti, L. Van Hove, Nucl. Phys. B30, 333 (1971).
14. J. Ballam et al., "Van Hove analysis of the reactions $\pi^{\pm}p \to \pi^{\pm}\pi^{+}\pi^{-}p$ at 16 GeV/c," SLAC-PUB-900.
15. S. Ljung and the Scandanavian Bubble Chamber Collaboration, Paper No. 327, contribution to this Conference.
16. F. Liu et al. (SLAC Streamer Chamber Group), SLAC-PUB-1047.
17. H. Harari, Mini-rapporteur report given at this Conference; H. Harari, Ann. Phys. (N.Y.) 63, 432 (1971); M. Davier and H. Harari, Phys. Letters 35B, 239 (1971); H. Harari and A. Schwimmer, SLAC-PUB-952.
18. M. Davier, Phys. Letters 40B, 369 (1972).
19. G. Chadwick et al., SLAC-PUB-1093.
20. R. Anderson et al., SLAC-PUB-1086.
21. R. Anderson et al., SLAC-PUB-1085.
22. H. Alvensleben et al. (DESY/MIT Group), "Photoproduction and forbidden decays of ϕ meson," paper contributed to this Conference.
23. H. Alvensleben et al. (DESY/MIT Group), "Determination of the photoproduction phase of the ϕ meson," Paper No. 794, contribution to this Conference.
24. Yu. M. Antipov et al. (CERN-IHEP Collaboration), Paper No. 442, contribution to this Conference.
25. V. D. Barger and D. B. Cline, Phenomenological theories of high energy scattering (Benjamin, New York, 1969).
26. R. Diebold et al., Preliminary data on $\pi^{\pm}$, $K^{\pm}$, $p^{\pm}$ on p scattering at 6 GeV/c
27. T. Lasinki et al., Nucl. Phys. B37, 1 (1972).
28. R. K. Carnegie et al., paper presented to this Conference.
29. D.R.O. Morrison, "Review of quasi two body reactions," CERN/D.PHII/Physics 71-10.
30. T. Ludlan et al., Phys. Rev. D2, 1234 (1970).
31. K. Barnham et al., Nucl. Phys. B25, 49 (1970).

32. P. Davis et al., LBL-36 (1971), submitted to Phys. Rev.
33. P. Baillon et al., Paper No. 624, contribution to this Conference.
34. K. Foley et al., Phys. Rev. 181, 1775 (1969).
35. a. F. Gilman et al., Phys. Letters 31B, 387 (1970).
    b. J. Deregel et al., Paper No. 603, contribution to this conference.
36. F. Halzen and C. Michael, Phys. Letters 36B, 367 (1971); A. deLesquen et al., Phys. Letters 40B, 277 (1972); G. Cozzika et al., Phys. Letters 40B, 281 (1972).
37. J. Ballam et al. (S-B-T Collaboration), SLAC-PUB-1092.
38. J. C. Vander Velde et al., Paper No. 451, contribution to this Conference.
39. Y. Oh et al., Paper No. 260, contribution to this conference.

41. V. Kruse et al., Paper No. 602, contribution to this Conference.
42. G. Ascoli et al., Paper No. 444, contribution to this Conference
43. R. Arnold et al., Paper No. 43, contribution to this Conference.
44. R. Barloutaud, Rapporteur: talk at the Oxford Conference on High Energy Physics and Elementary Particles.
45. Y. Goldschmidt-Clermont, Mini-rapporteur report at this Conference.
46. A. Filippas et al., Paper No. 505, contribution to this Conference.
47. H. H. Bingham et al., U. C. Berkeley Cosmic Ray Group Preprint (private communication).
48. J. Ballam et al. (S-B-T Collaboration).
49. J. Ballam et al., Paper No. 111 submitted to the Fourth International Symposium on Electron and Photon Interactions at High Energies, 1969; and H. H. Bingham et al., Bull. Am. Phys. Soc. 17, 469 (1972).

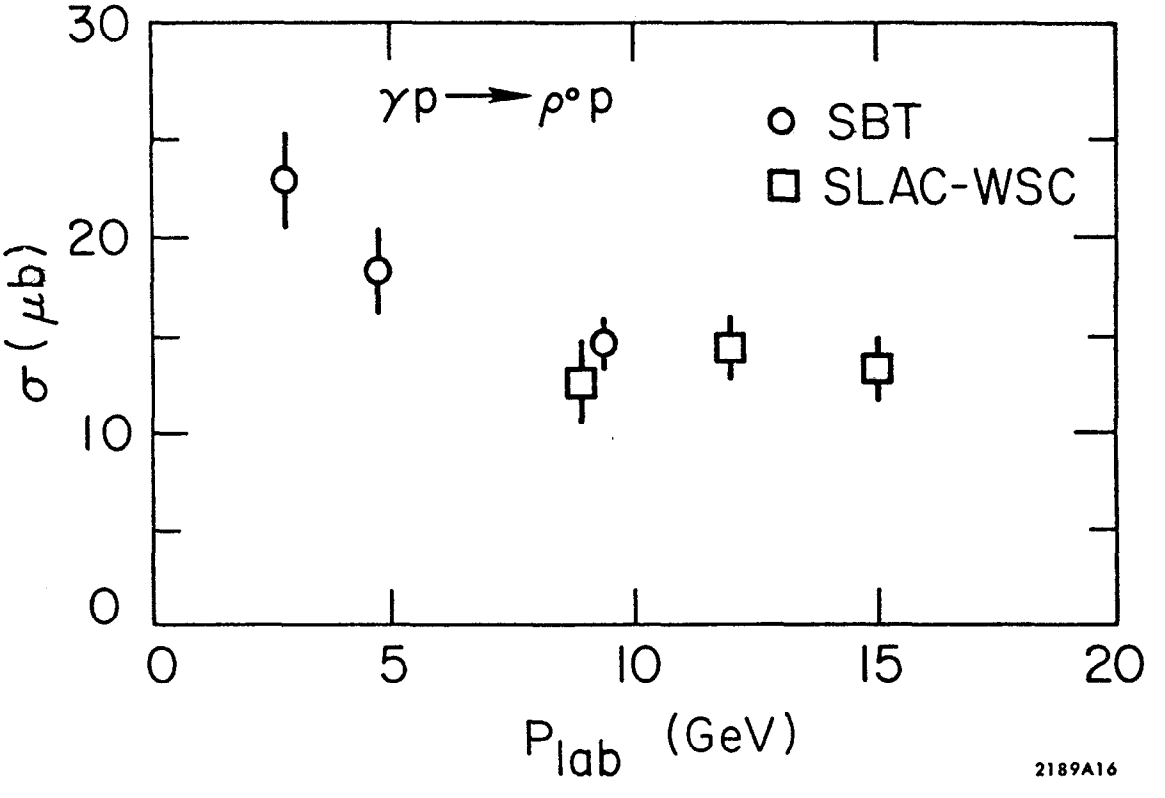

FIG. 1--The cross section for $\gamma p \rightarrow \rho^{o} p$ as a function of energy.

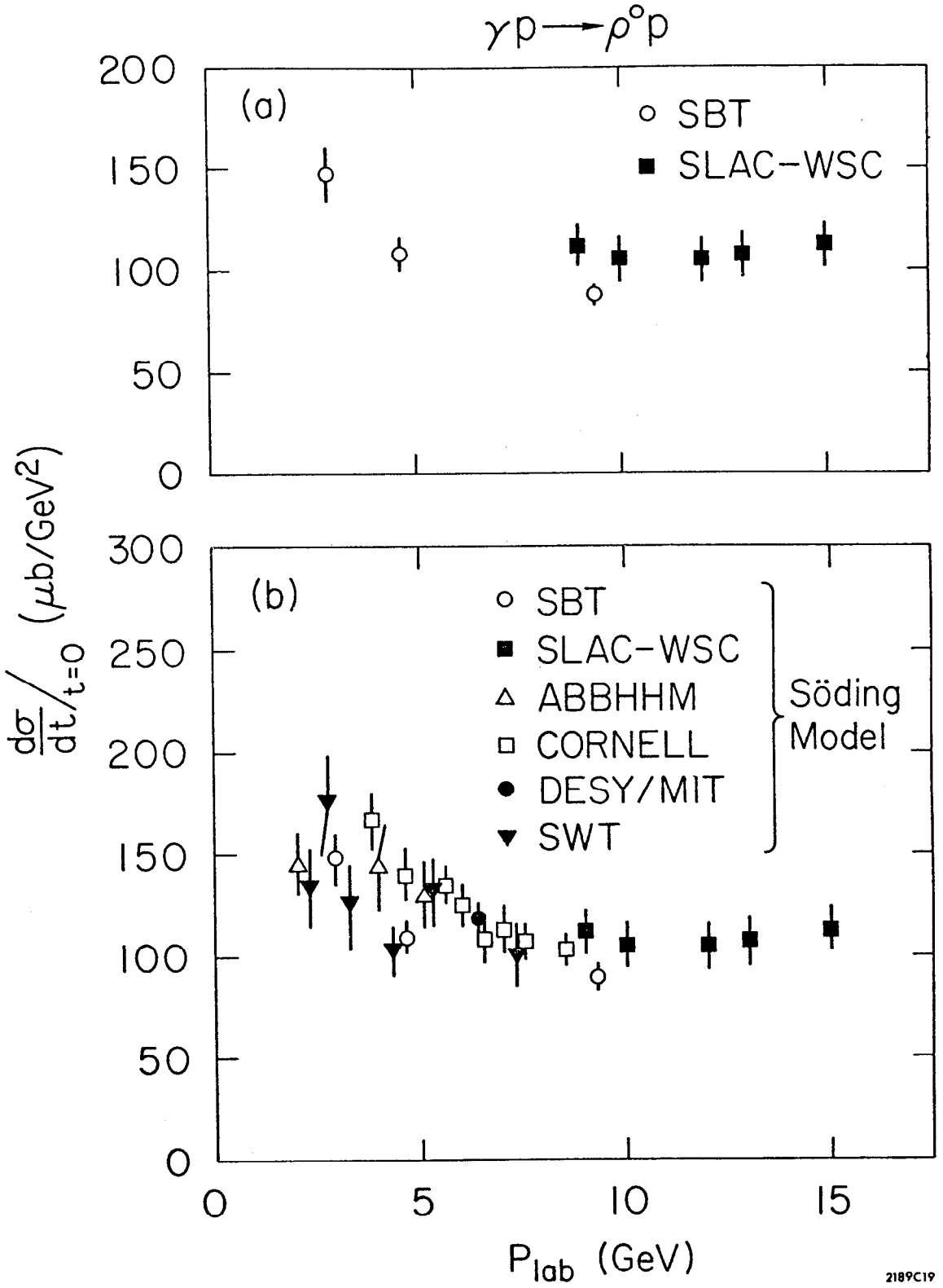

FIG. 2--The forward differential cross section for the reaction $\gamma p \rightarrow \rho^{o} p$ as a function of energy, (a) for new data presented to this conference, and (b) for all available data on the reaction. All cross sections were analyzed using the Söding model.

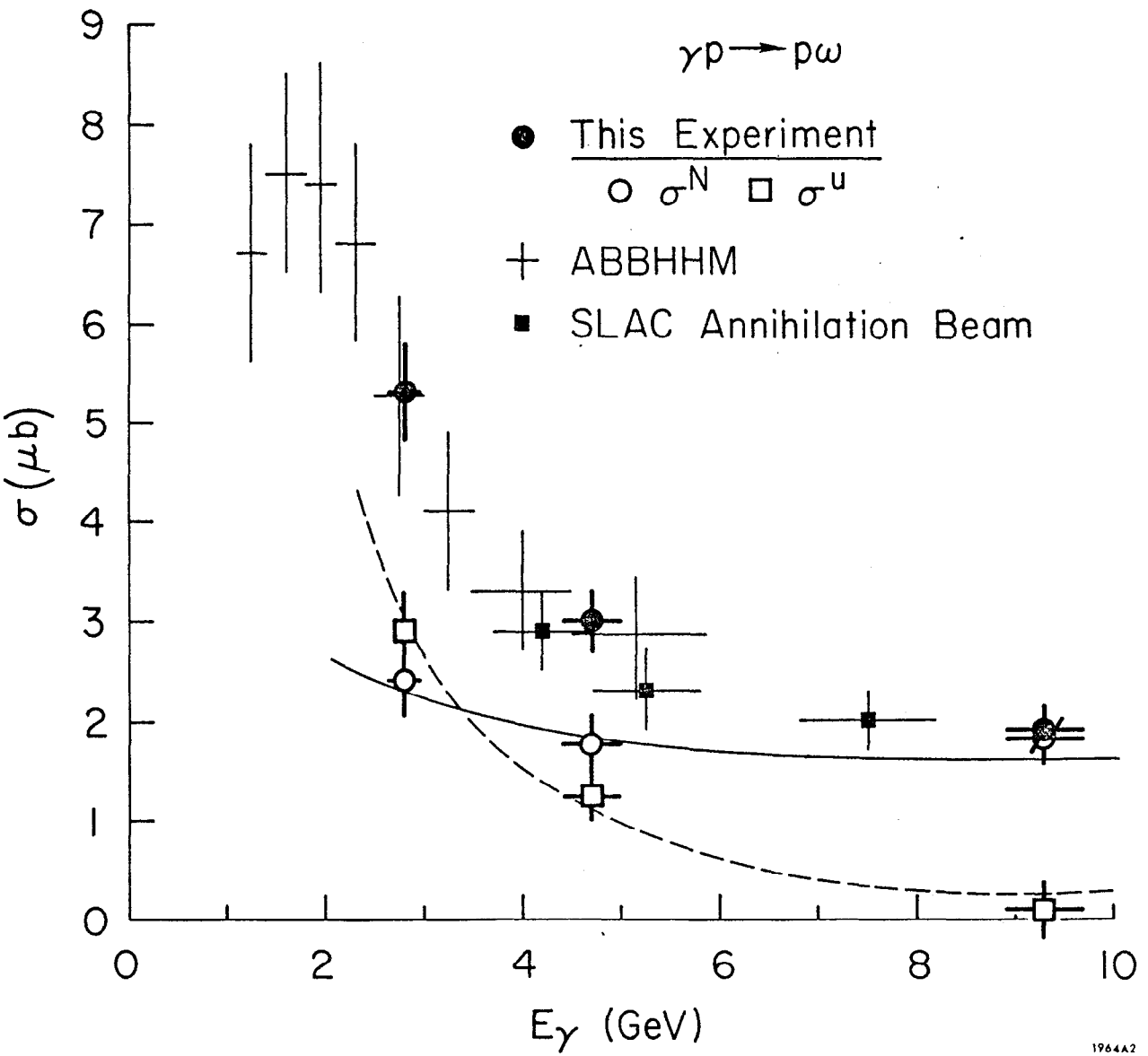

FIG. 3--The cross section for $\gamma p \rightarrow \omega p$ as a function of energy, also showing the natural parity (σ^N) and unnatural parity (σ^U) contributions at 2.8, 4.7 and 9.3 GeV.

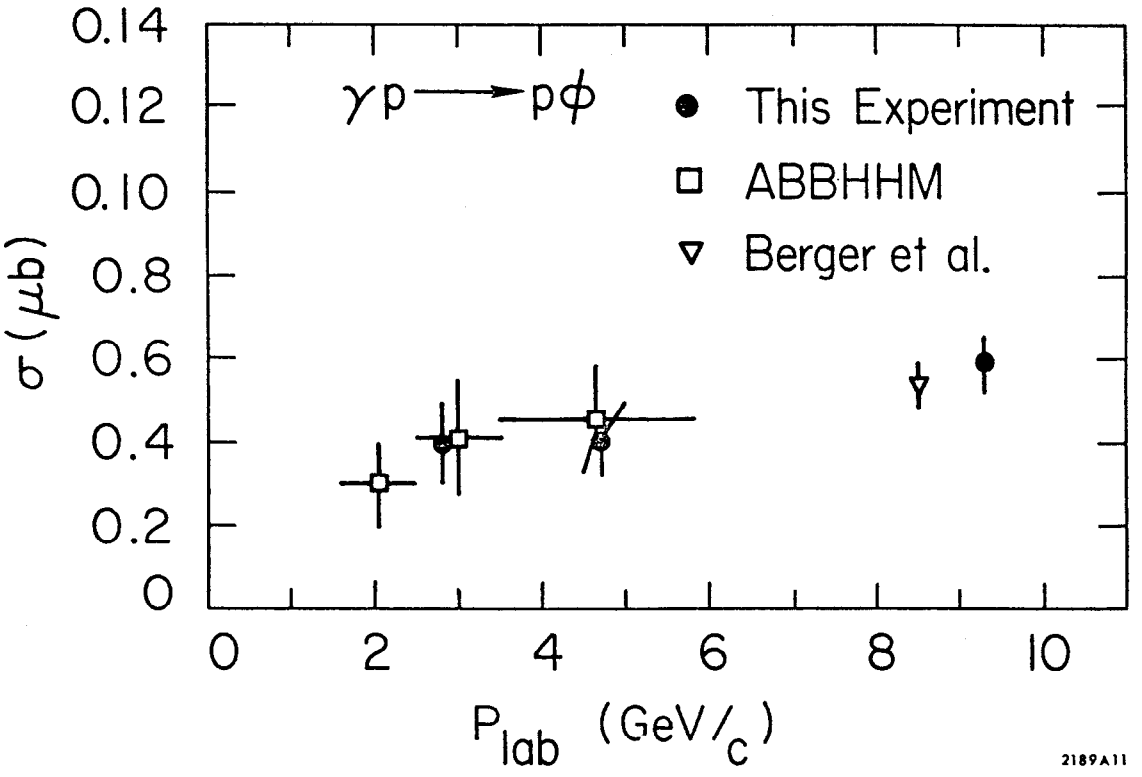

FIG. 4--The cross section for the reaction $\gamma p \rightarrow \phi p$ as a function of energy.

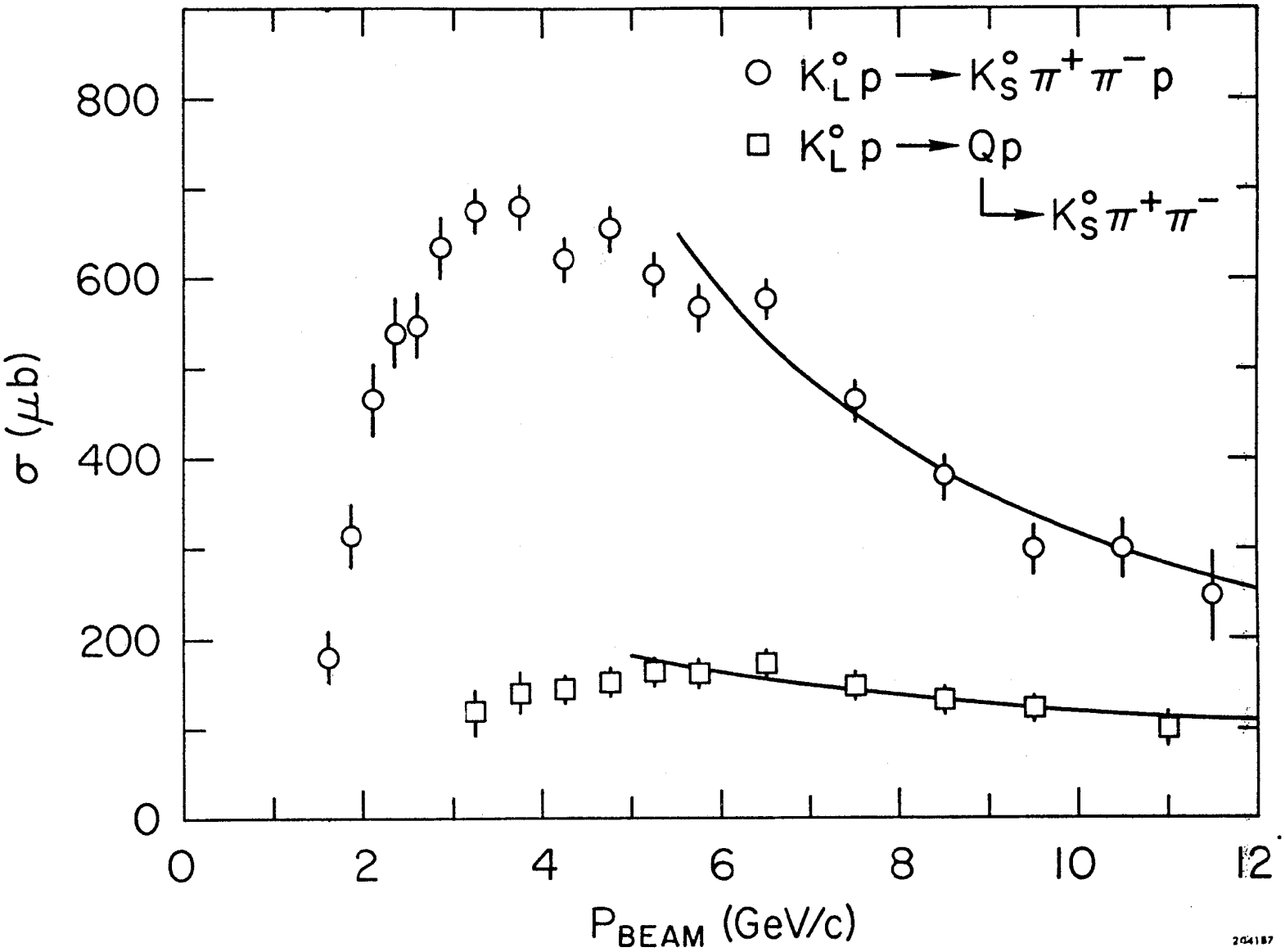

FIG. 5--The cross sections for the process $K_L^o p \rightarrow K_S^o \pi^+ \pi^- p$, and the sub-process $K_L^o p \rightarrow Q^o p$, as a function of energy.

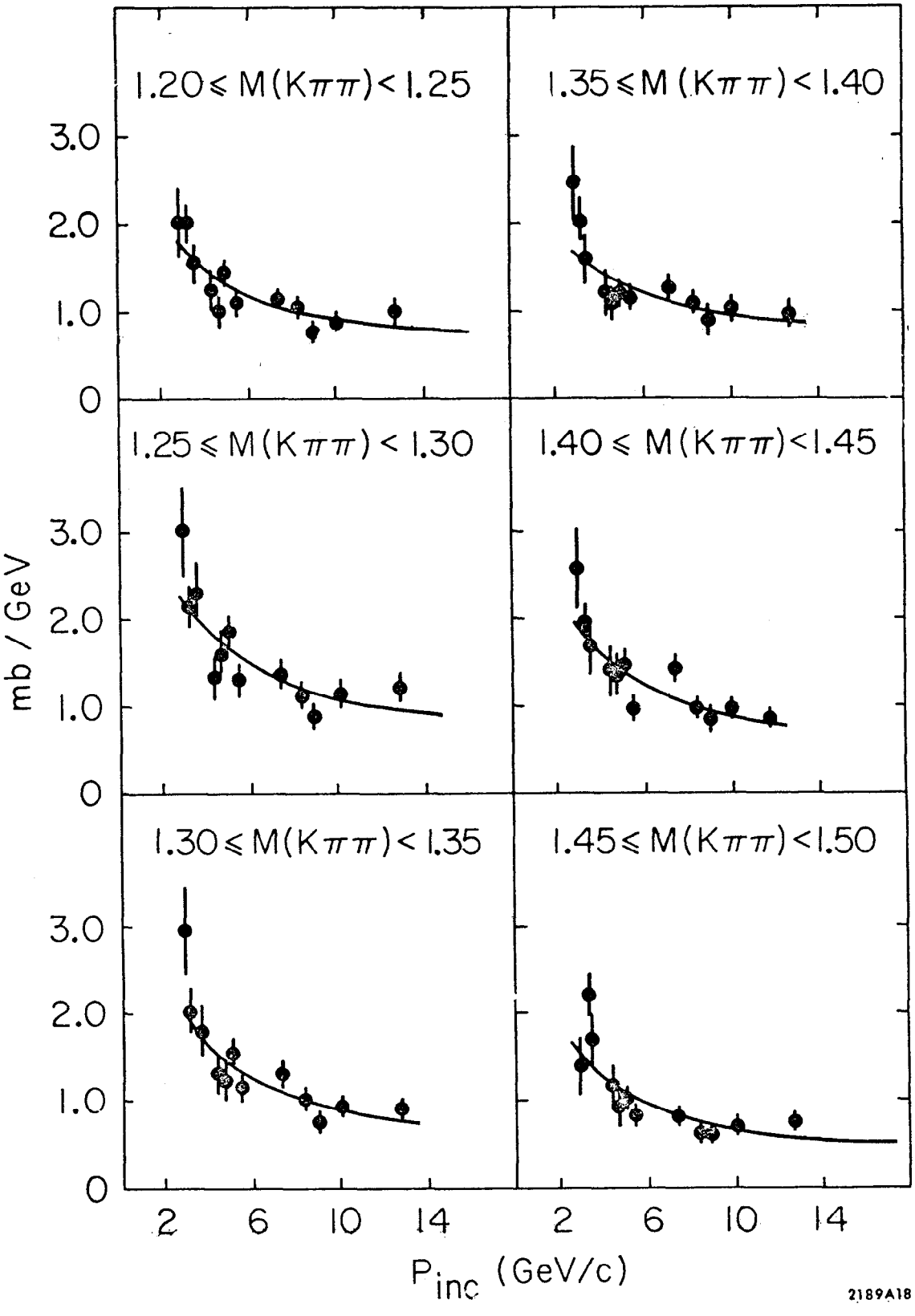

FIG. 6--The cross section for $K^+p \rightarrow Q^+p$ as a function of energy for six regions of ($K\pi\pi$) mass from (1200 - 1500) MeV.

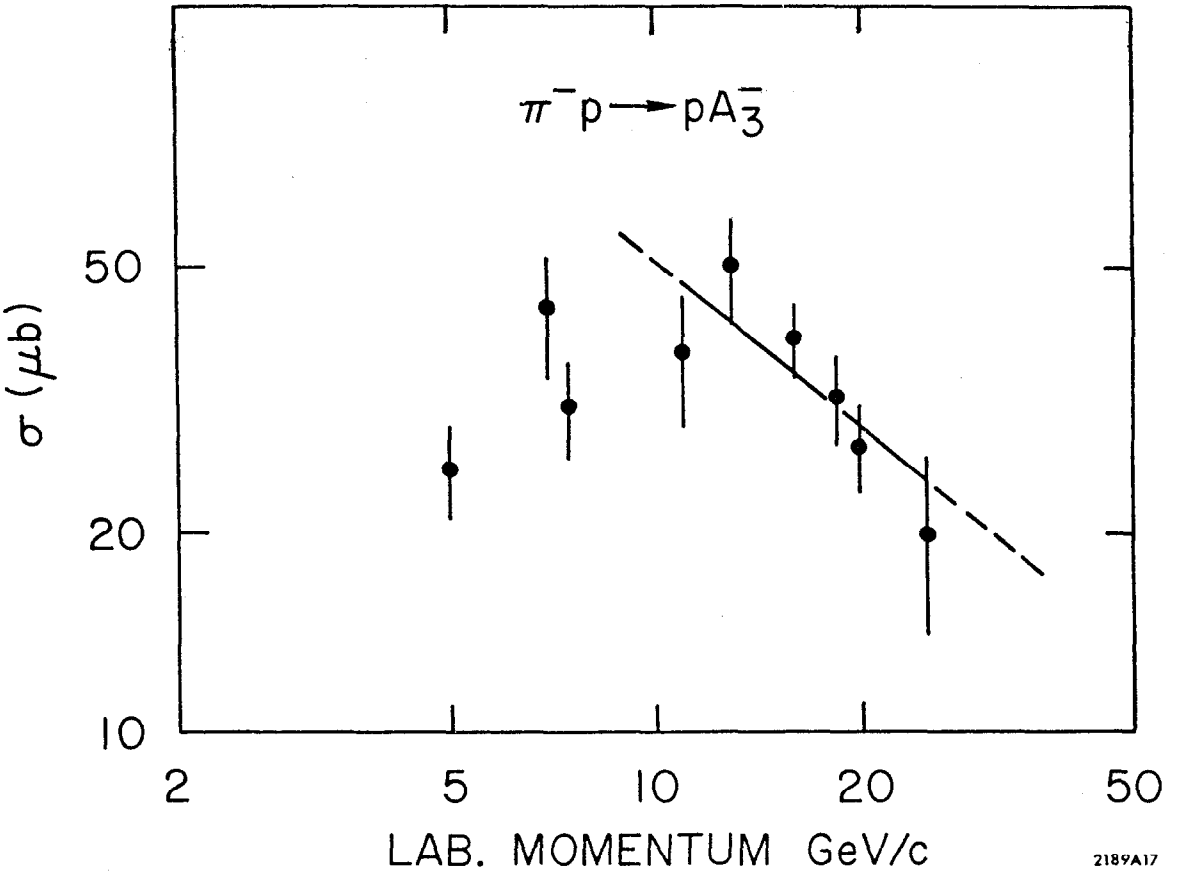

FIG. 7--The cross section for $\pi^- p \rightarrow \bar{A}_3 p$ as a function of energy.

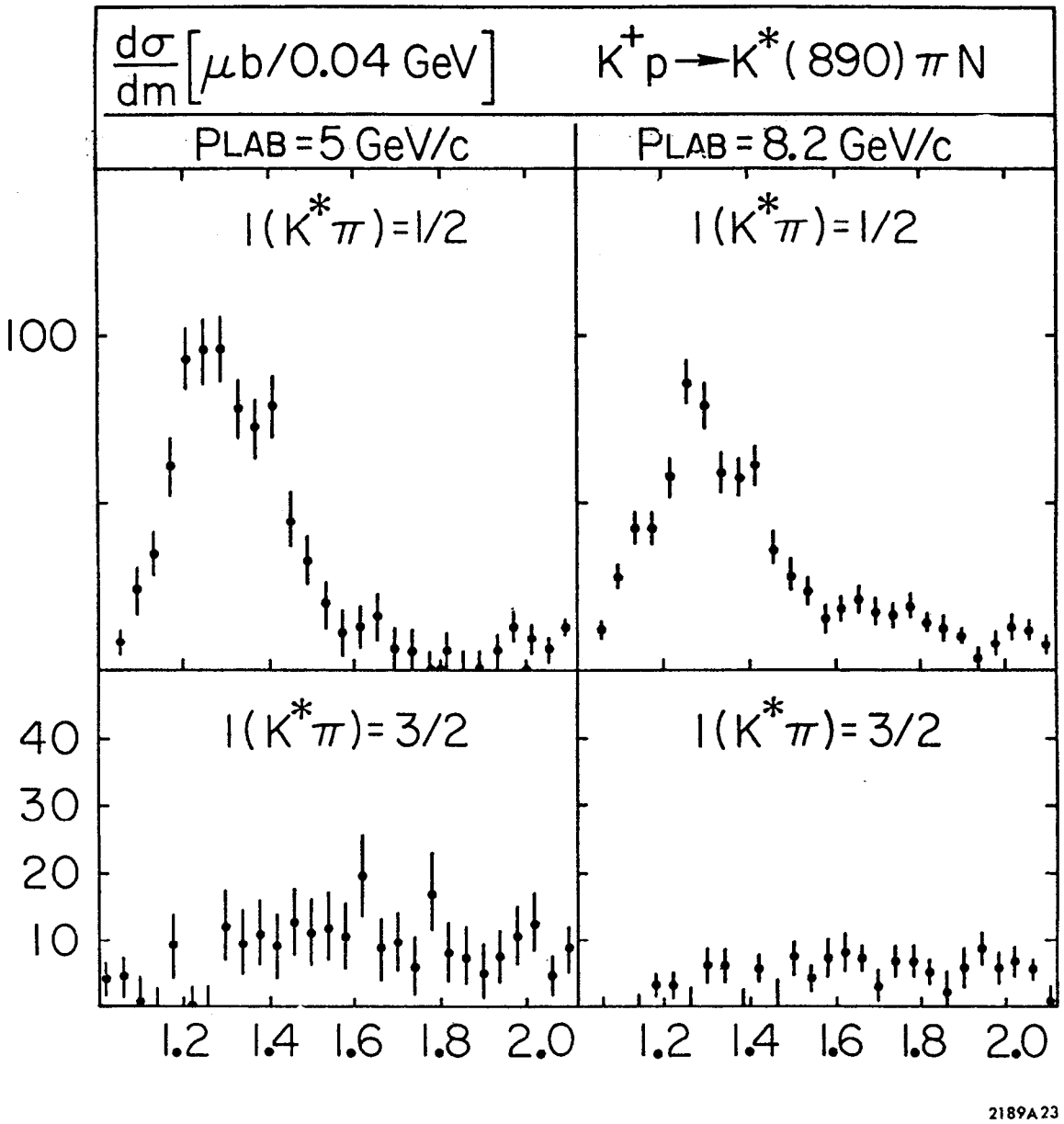

FIG. 8--The mass distribution for the $K^*\pi$ system from the reaction $K^+p \rightarrow K^*(890)\pi N$ at 5 GeV/c and 8.2 GeV/c, for I=1/2 and I=3/2 amplitudes separately.

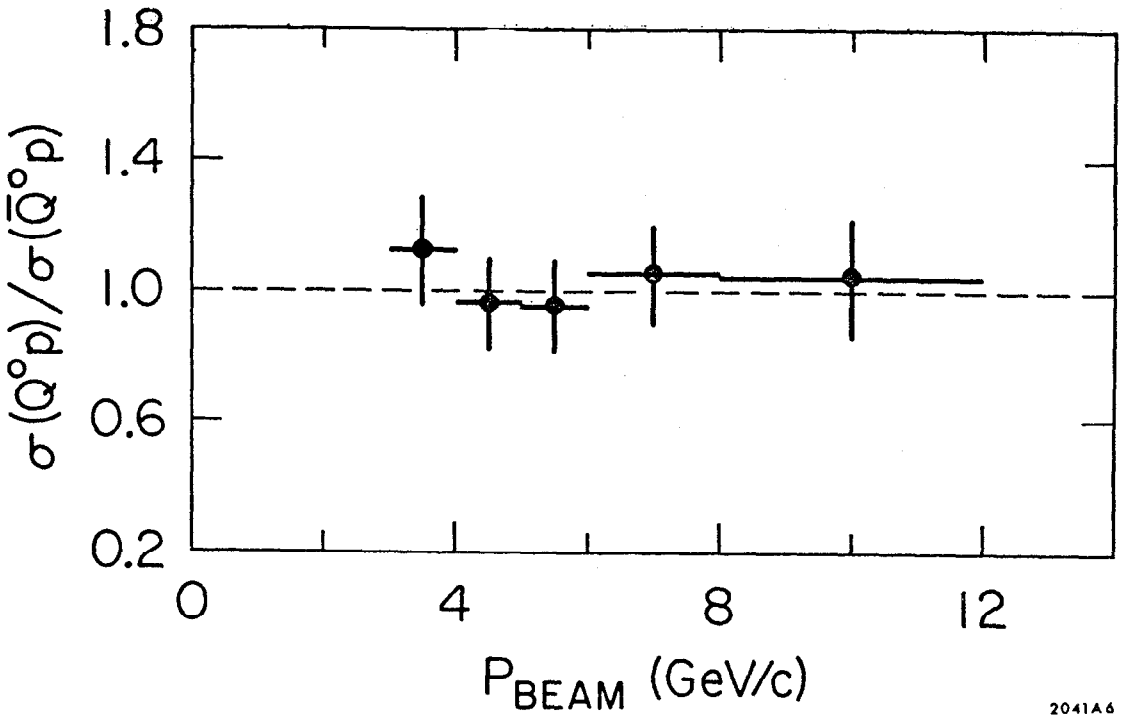

FIG. 9--The ratio of the cross sections $K^{o}p \rightarrow Q^{o}p$ and $\bar{K}^{o}p \rightarrow \bar{Q}^{o}p$ as a function of momentum.

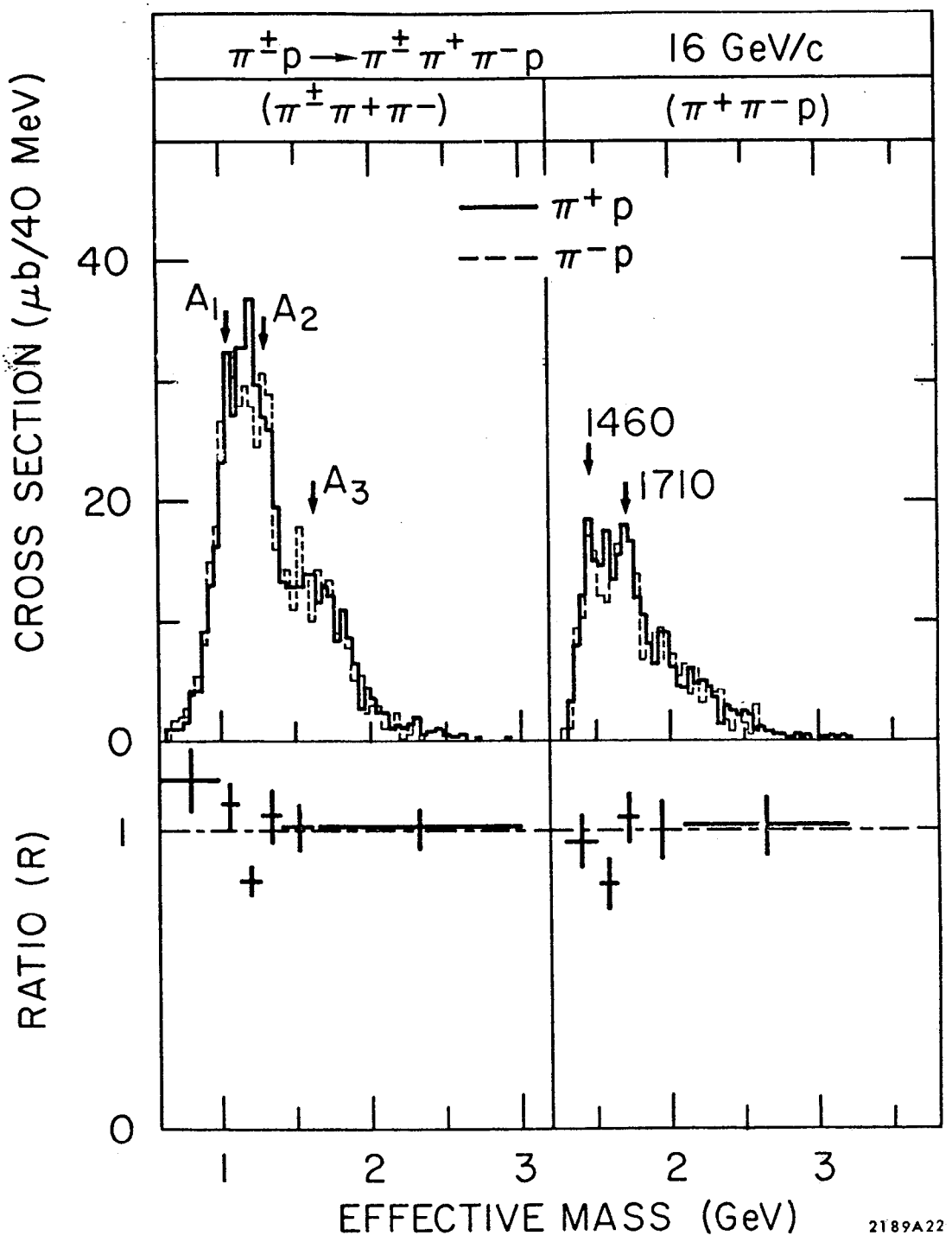

FIG. 10--The mass distribution for $(\pi^{\pm}\pi^{+}\pi^{-})$ and $(p\pi^{+}\pi^{-})$ from the reactions $\pi^{\pm}p \rightarrow \pi^{\pm}\pi^{+}\pi^{-}p$ at 16 GeV/c. Below, the ratio of the mass distributions for the $\pi^{+}p$ and $\pi^{-}p$ reactions are also shown.

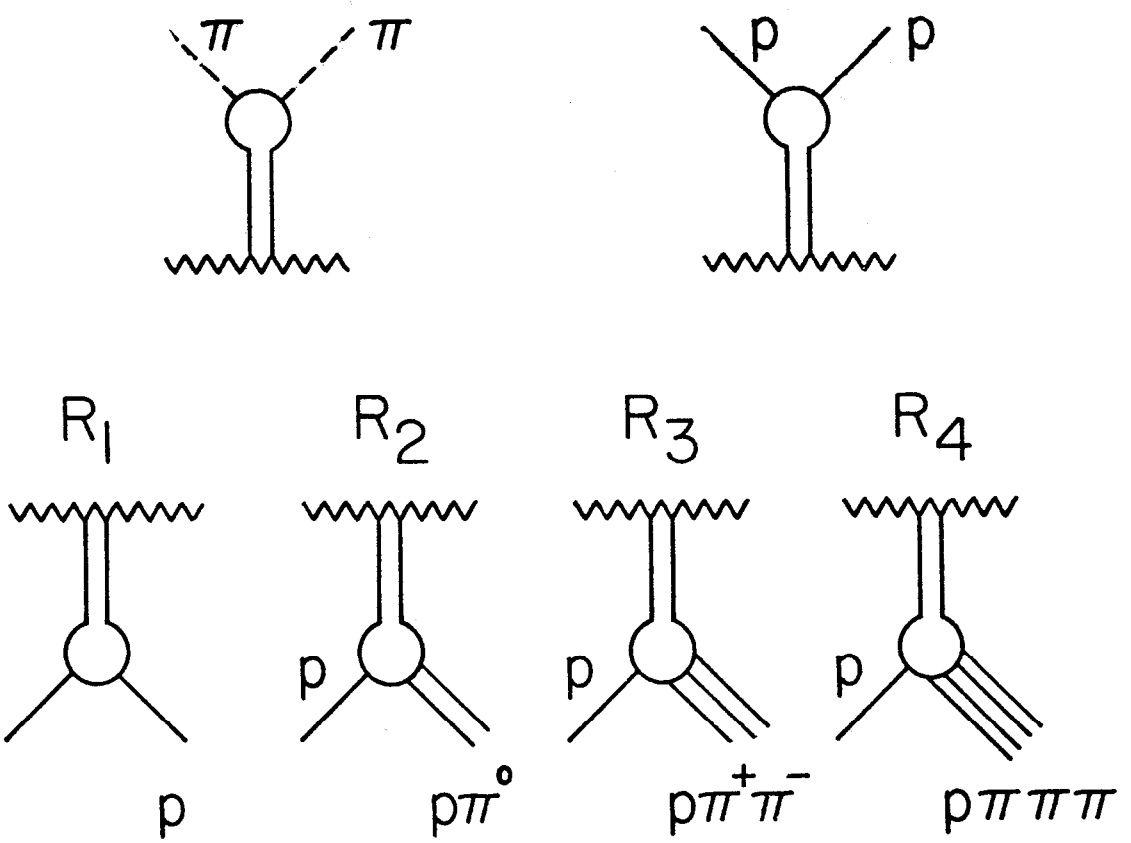

FIG. 11--A schematic of diffractive reactions studied in a test of factorization. The ratios $R_1 - R_4$ refer to the ratio of the cross sections of reactions when the top two vertices (pion and proton elastic scattering), are joined successively to the bottom four vertices, representing proton diffraction into a proton plus zero, one, two or three pions respectively.

$$\left(\text{e.g.,} \quad R_1 = \left[\frac{\sigma(\pi p \to \pi p)}{\sigma(pp \to pp)}\right], \quad R_2 = \left[\frac{\sigma(\pi p \to \pi p \pi)}{\sigma(pp \to pp\pi)}\right]\right)$$

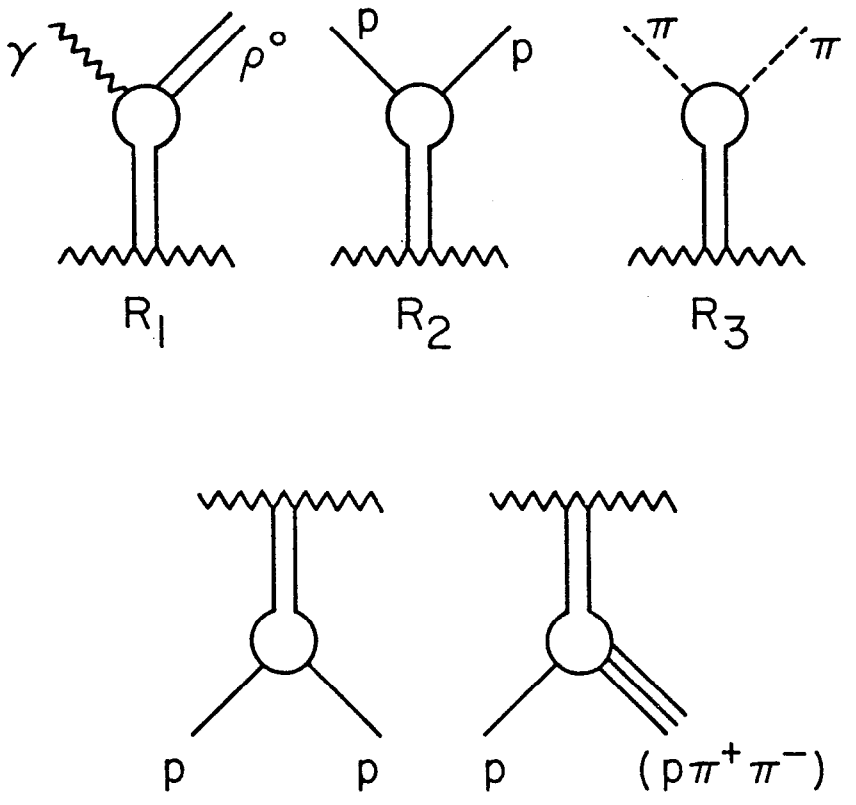

FIG. 12--A schematic of diffractive reactions studied in a test of factorization. The ratio R_1, R_2, R_3 refers to the ratio of the cross sections when each of the upper vertices ($\gamma \rightarrow \rho^0$, $p \rightarrow p$ or $\pi \rightarrow \pi$), is connected with the two lower vertices, representing proton diffraction into a proton or a ($p\pi\pi$) system, respectively.

$$\left(\text{e.g.,} \quad R_1 = \frac{\sigma(\gamma p \rightarrow \rho p)}{\sigma(\gamma p \rightarrow \rho p \pi\pi\pi)} \,, \quad R_2 = \frac{\sigma(pp \rightarrow pp)}{\sigma(pp \rightarrow pp\pi\pi\pi)} \right.$$

$$\left. R_3 = \frac{\sigma(\pi p \rightarrow \pi p)}{\sigma(\pi p \rightarrow \pi p \pi\pi\pi)} \right)$$

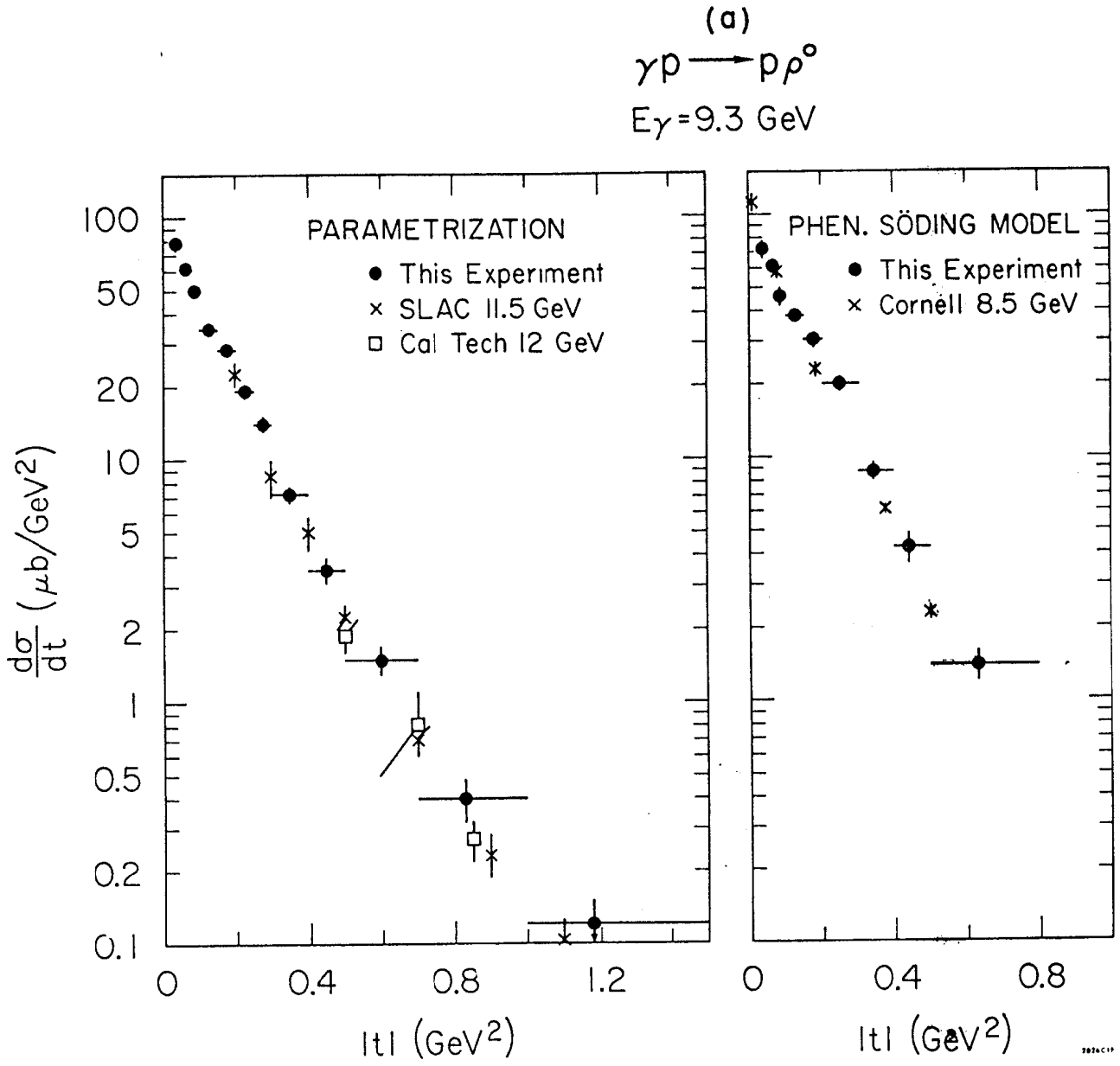

FIG. 13--The differential cross section for photoproduction of rho meson; (a) at 9.3 GeV from the S-B-T laser experiment Ref. 3; and (b) at several energies from (9 - 16) GeV from the SLAC wire spark chamber experiment Ref. 6.

FIG. 13--continued.

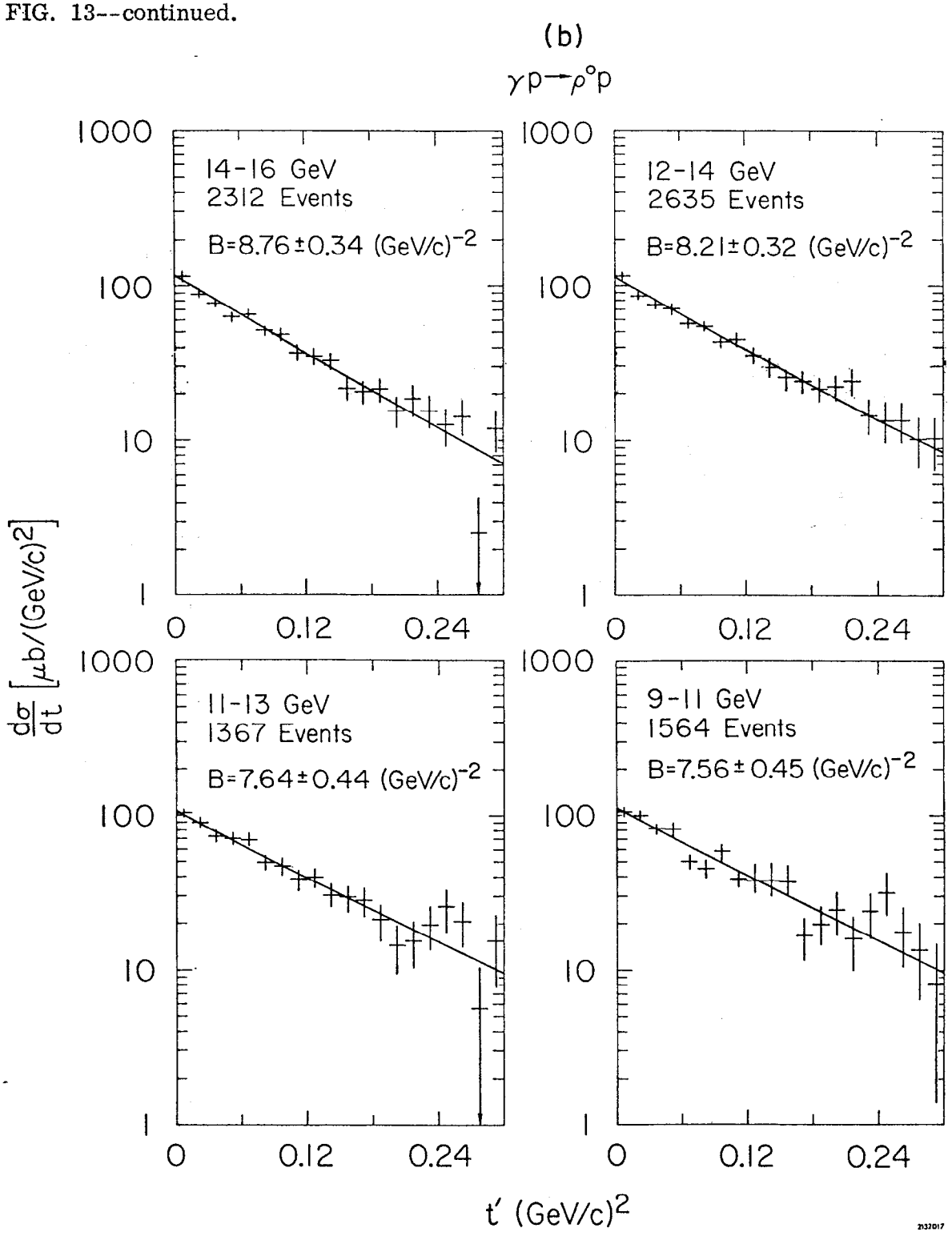

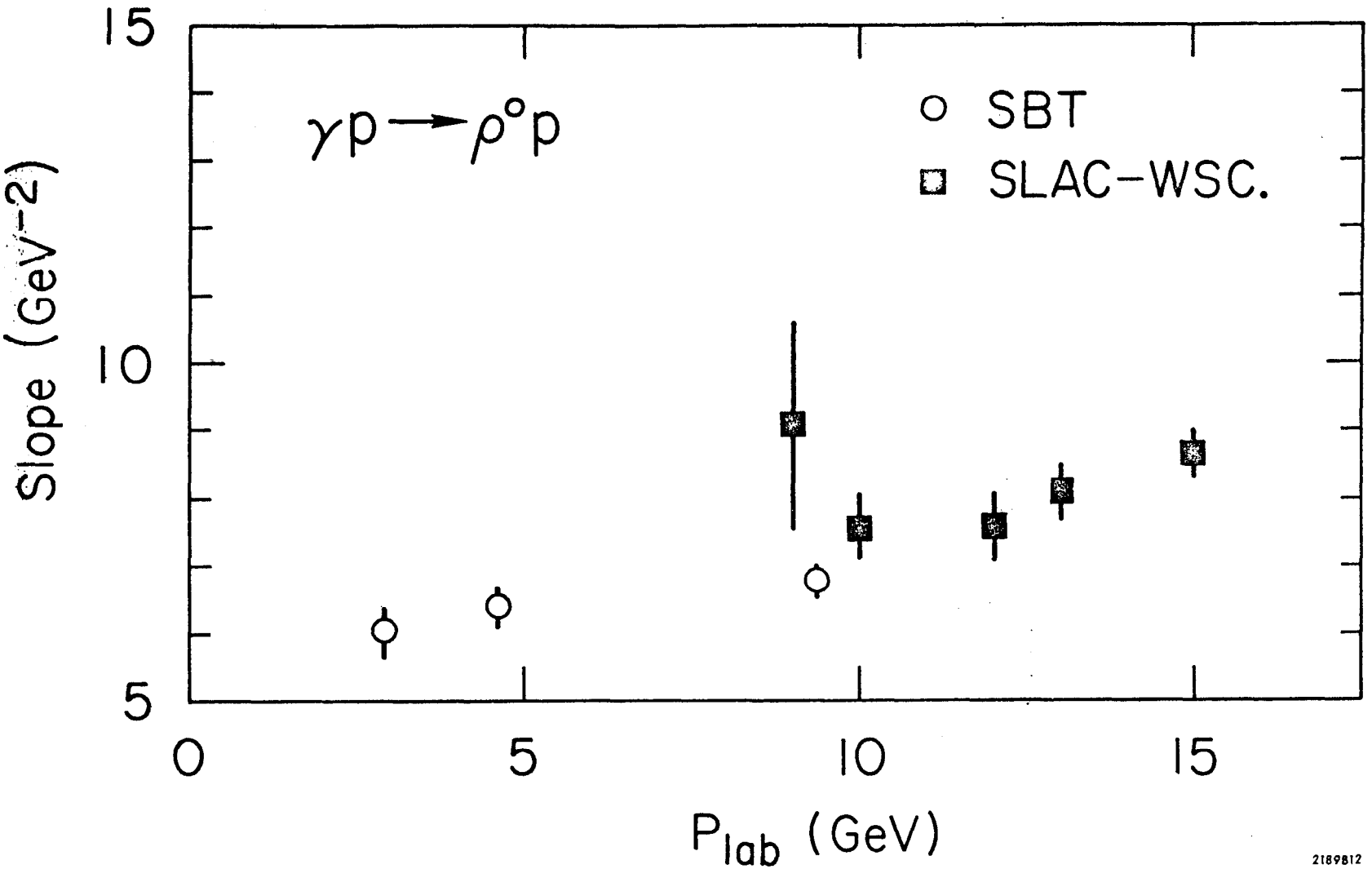

FIG. 14--The slope of the differential cross section for $\gamma p \rightarrow \rho^{o} p$ as a function of energy, for new cross sections presented to the Conference. The data were analyzed using the Söding model for the s- and t-dependence of the dipion system.

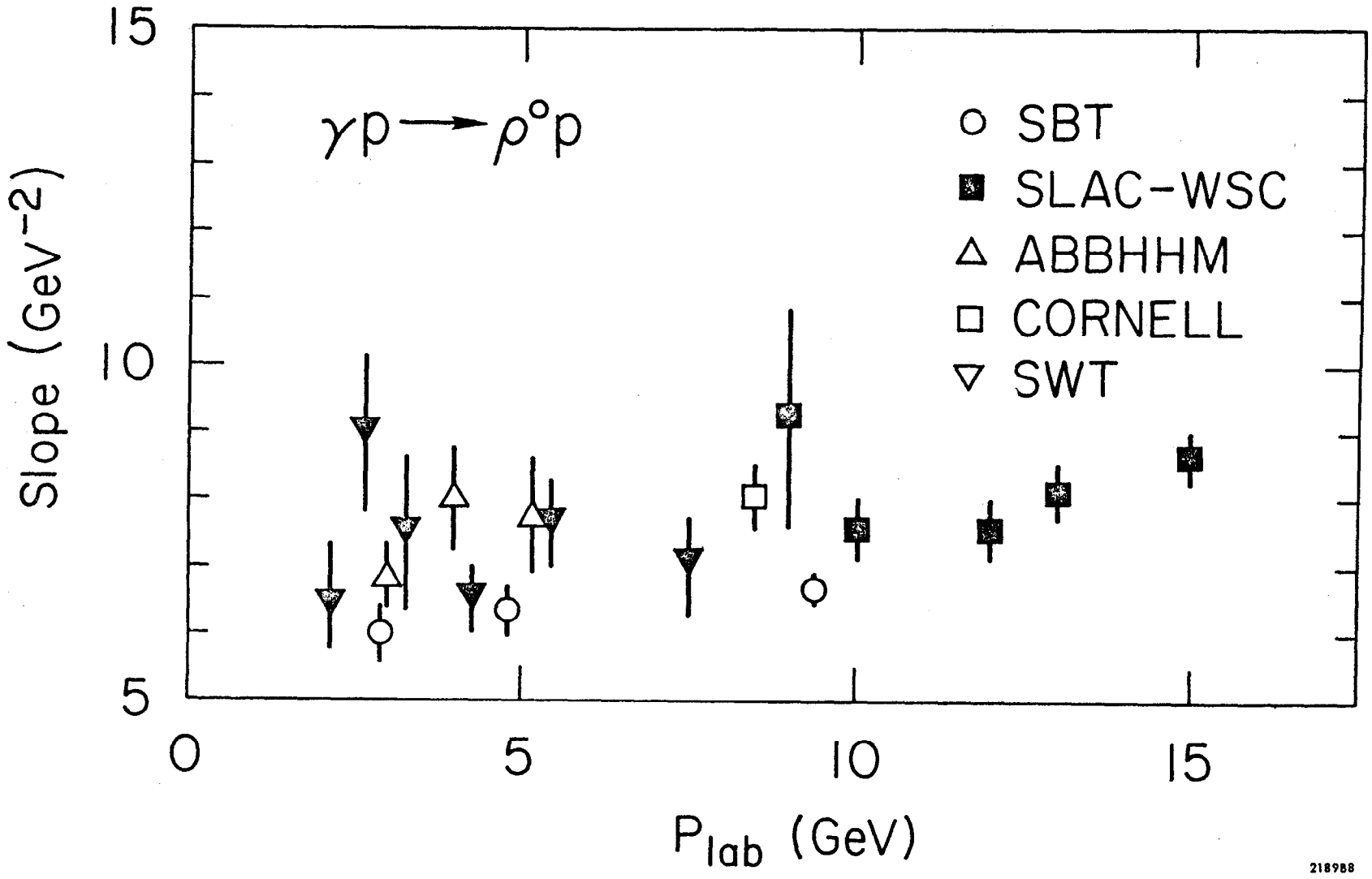

FIG. 15--The slope of the differential cross section for $\gamma p \rightarrow \rho^{\circ} p$ as a function of energy for all available data analyzed using the Söding model.

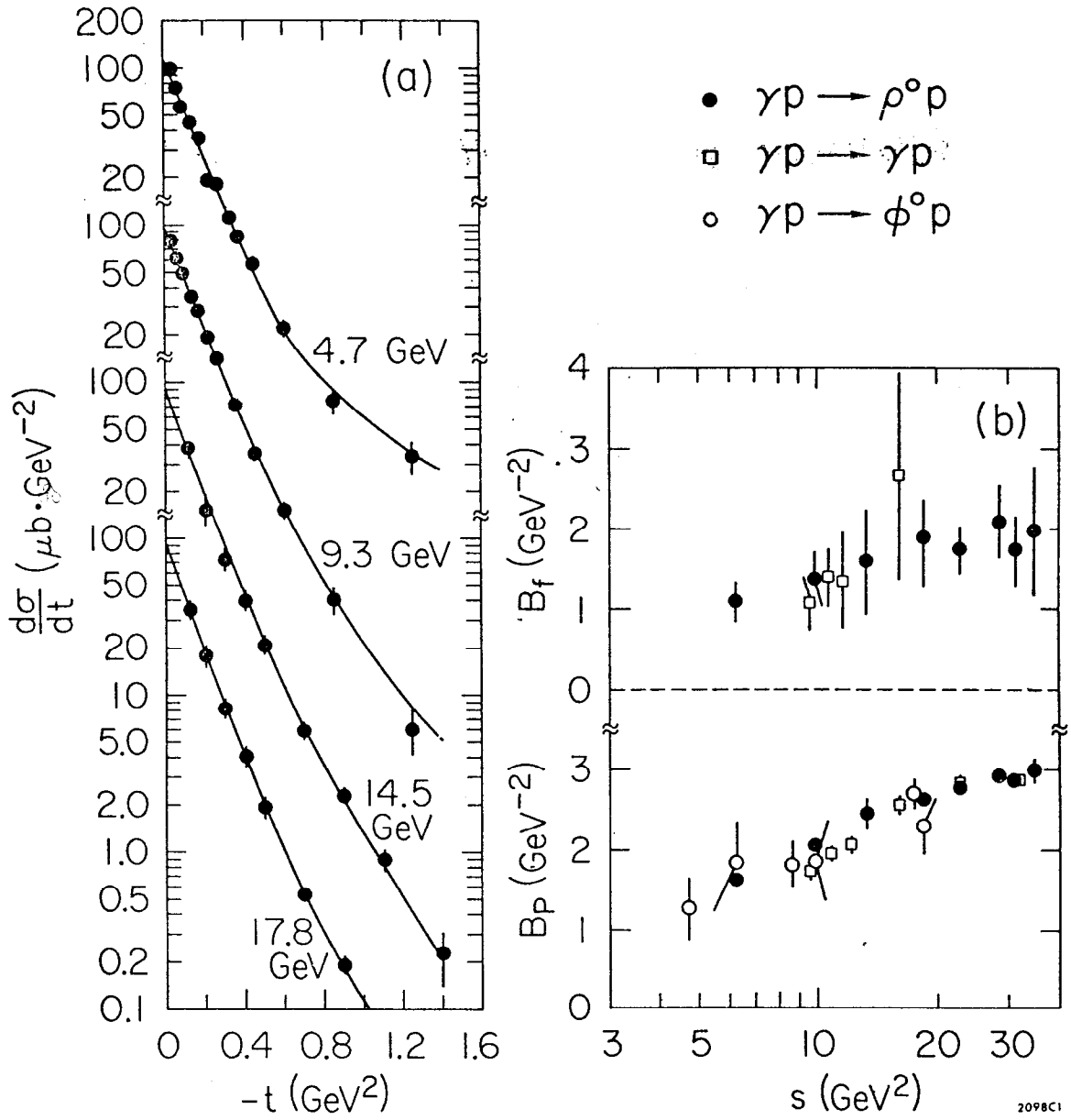

FIG. 16--(a) Fits of $d\sigma/dt$ of ρ^0 photoproduction to sum of P and f exchange, utilizing Dual Absorption Model. (b) P and f exchange amplitude slopes as obtained from fits of $d\sigma/dt$. The errors in $\gamma p \rightarrow \rho^0 p$ are statistical only. The systematic uncertainties are estimated to be ±10%.

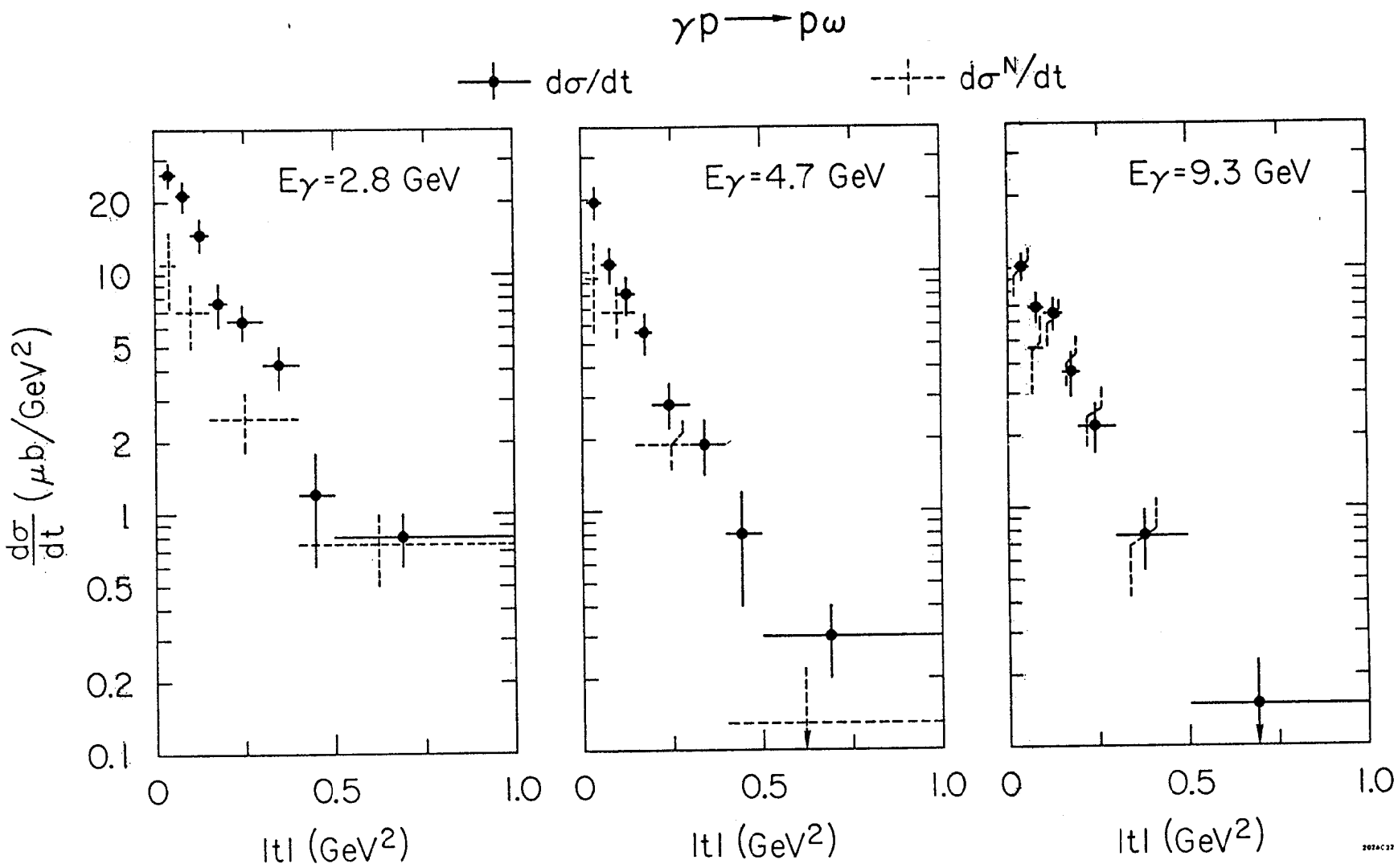

FIG. 17--The differential cross section for the reaction $\gamma p \rightarrow \omega p$ at 2.8, 4.7 and 9.3 GeV (ϕ), and the natural parity contribution to the differential cross section ($-\dagger-$).

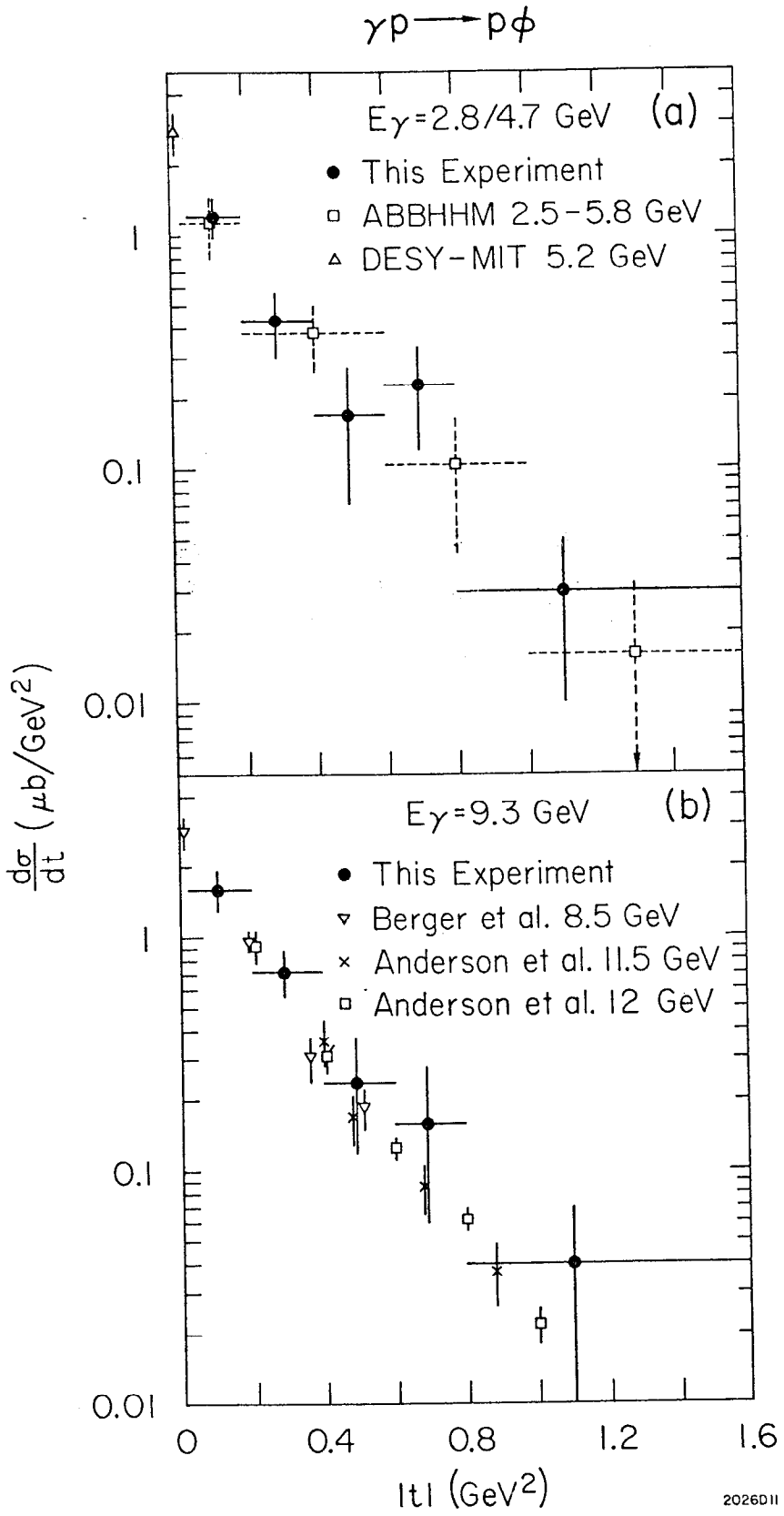

FIG. 18--Reaction $\gamma p \rightarrow p\phi$ at 2.8, 4.7 and 9.3 GeV. Differential cross section: (a) 2.8 and 4.7 GeV data combined; (b) 9.3 GeV; (c) shows the experimental values for $d\sigma/dt$ for ϕ photoproduction at 12 GeV as a function of $-t$ from 0.2 to 1.0 $(GeV/c)^2$. See Refs. 3 and 20 for description of curves and references to other data. (d) shows the same curves and points as in (c) with the addition of Cornell and DESY results. Agreement of all data is excellent.

FIG. 18--continued.

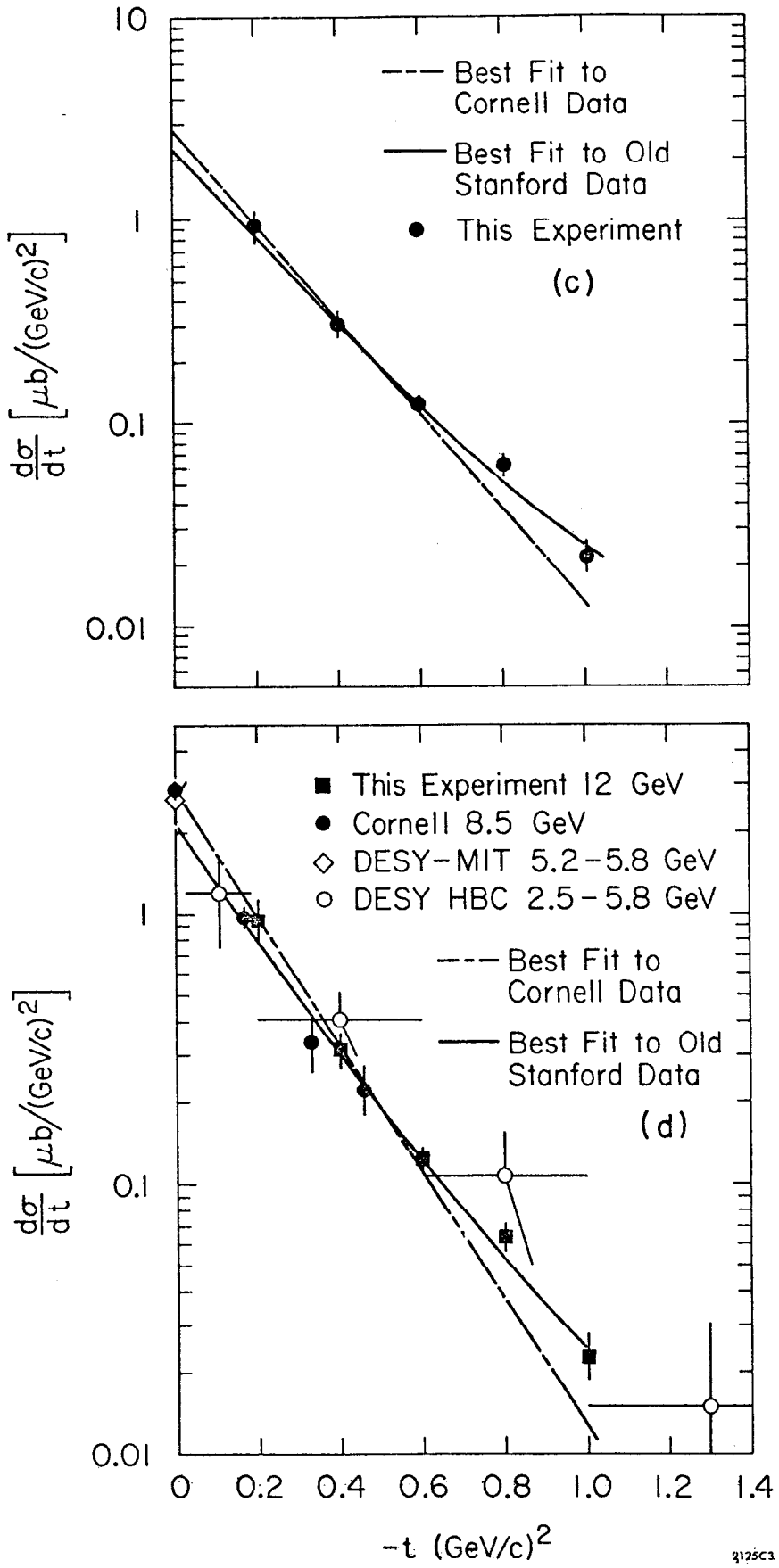

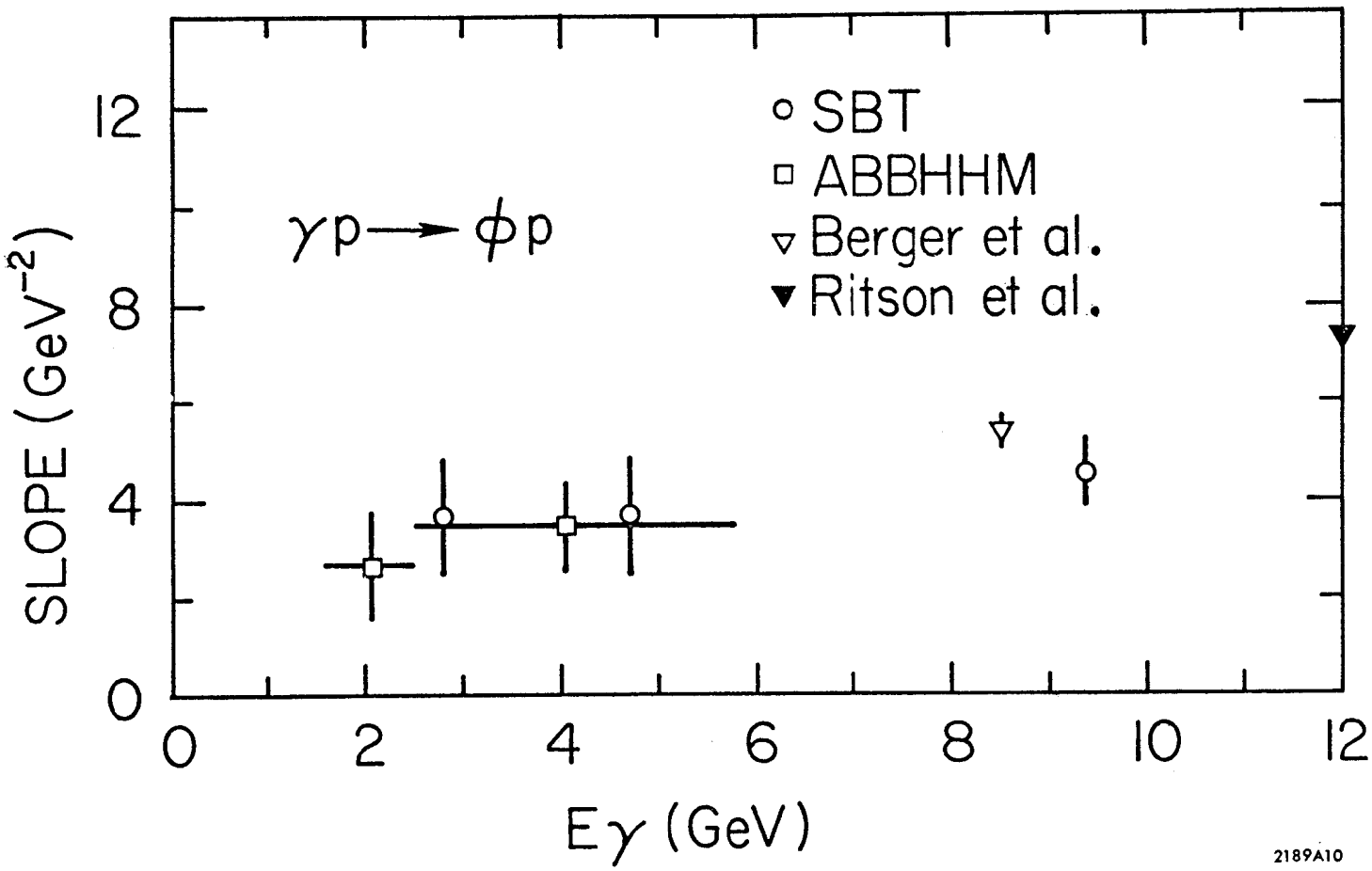

FIG. 19--The slope of the differential cross section for $\gamma p \rightarrow \phi p$ as a function of energy.

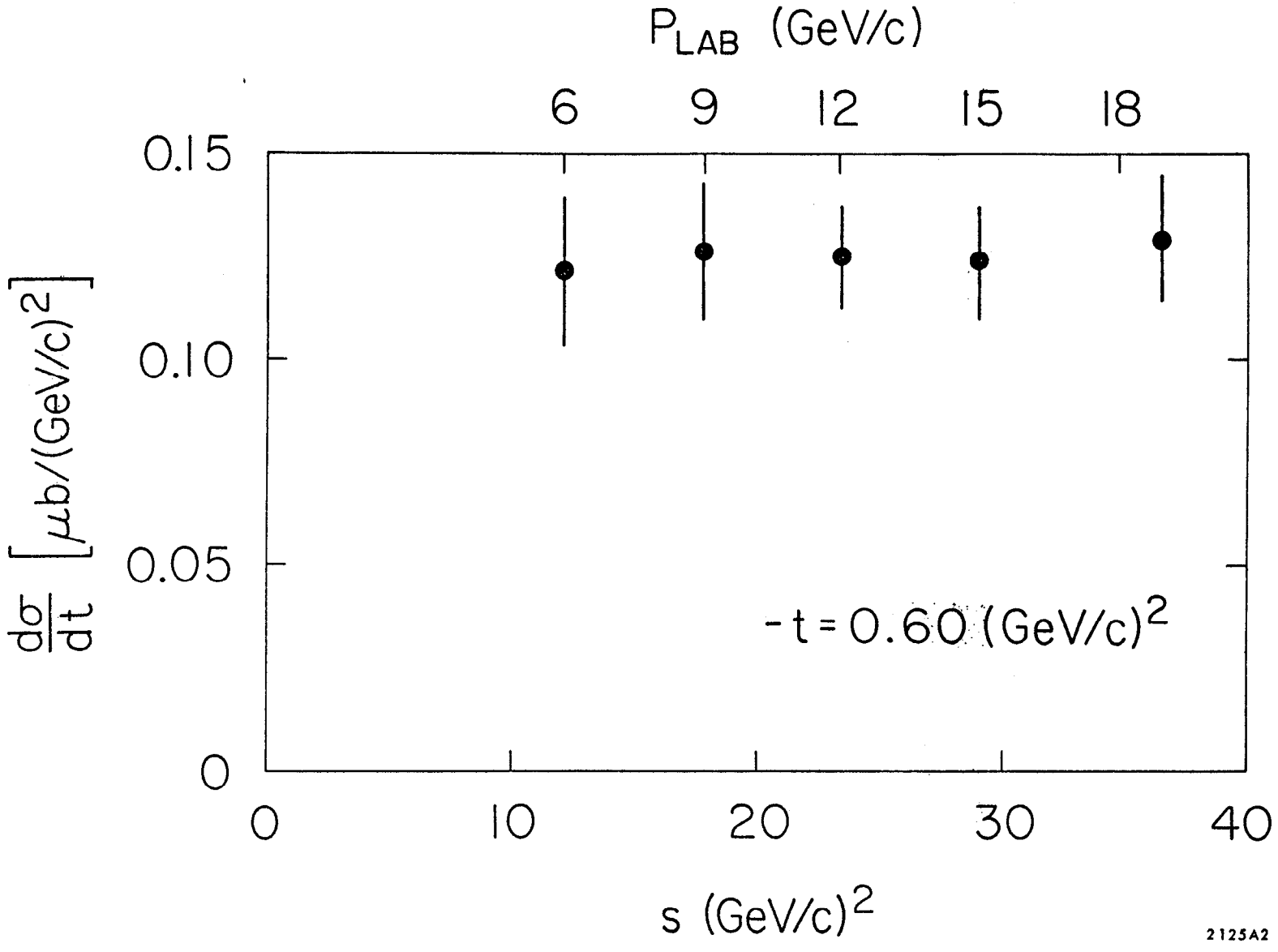

FIG. 20--The s-dependence of the differential cross section for $\gamma p \rightarrow \phi p$ at a momentum transfer $t = 0.6$ GeV^2. The data indicate no shrinkage of the ϕ cross section, at this value of t.

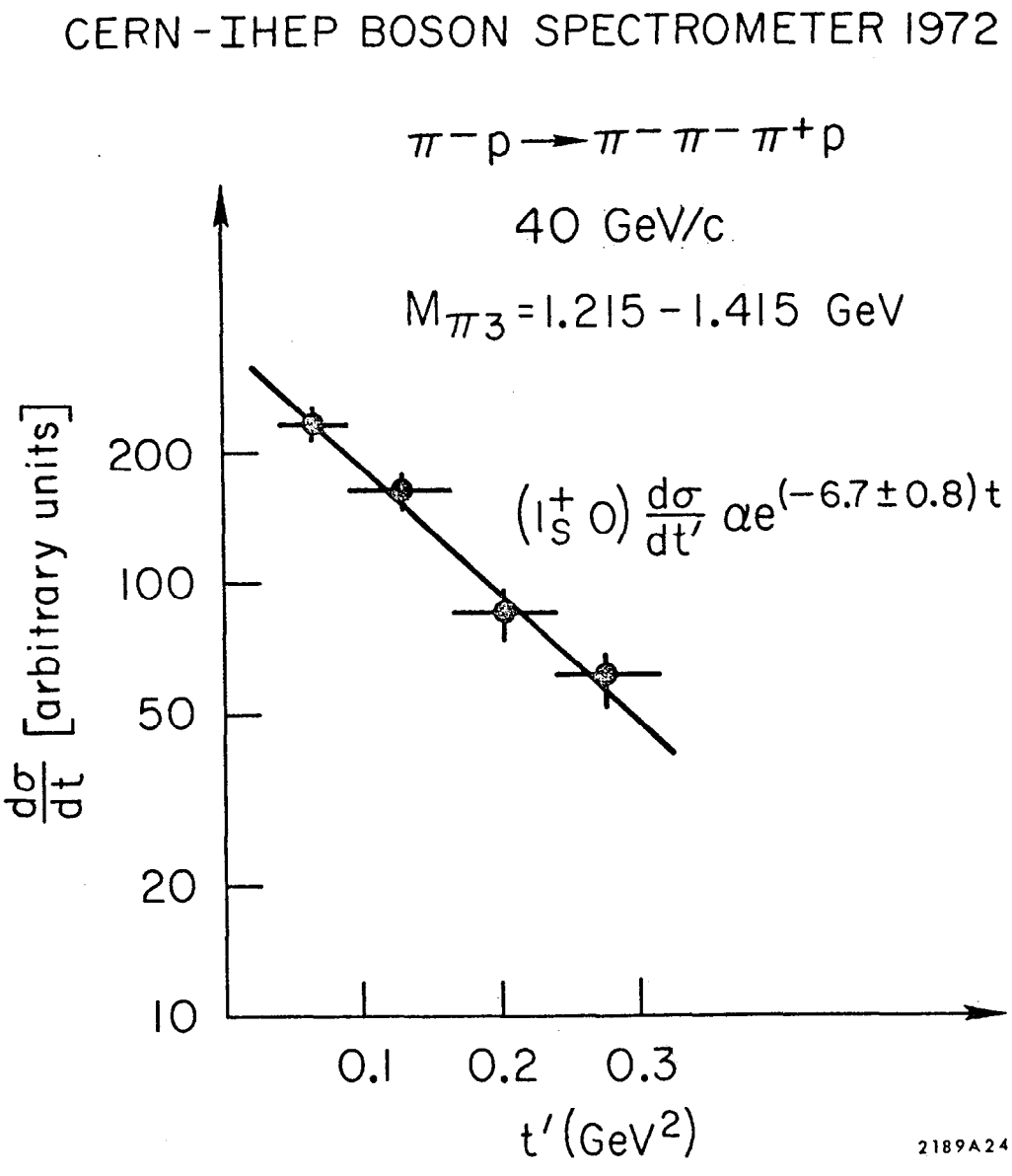

FIG. 21--The differential cross section for $\pi^- p \rightarrow A^- p$ at 40 GeV/c. The A_1 region is here defined as the 1^+ spin parity amplitude for $1.215 \leq M(3\pi) \leq 1.415$ GeV.

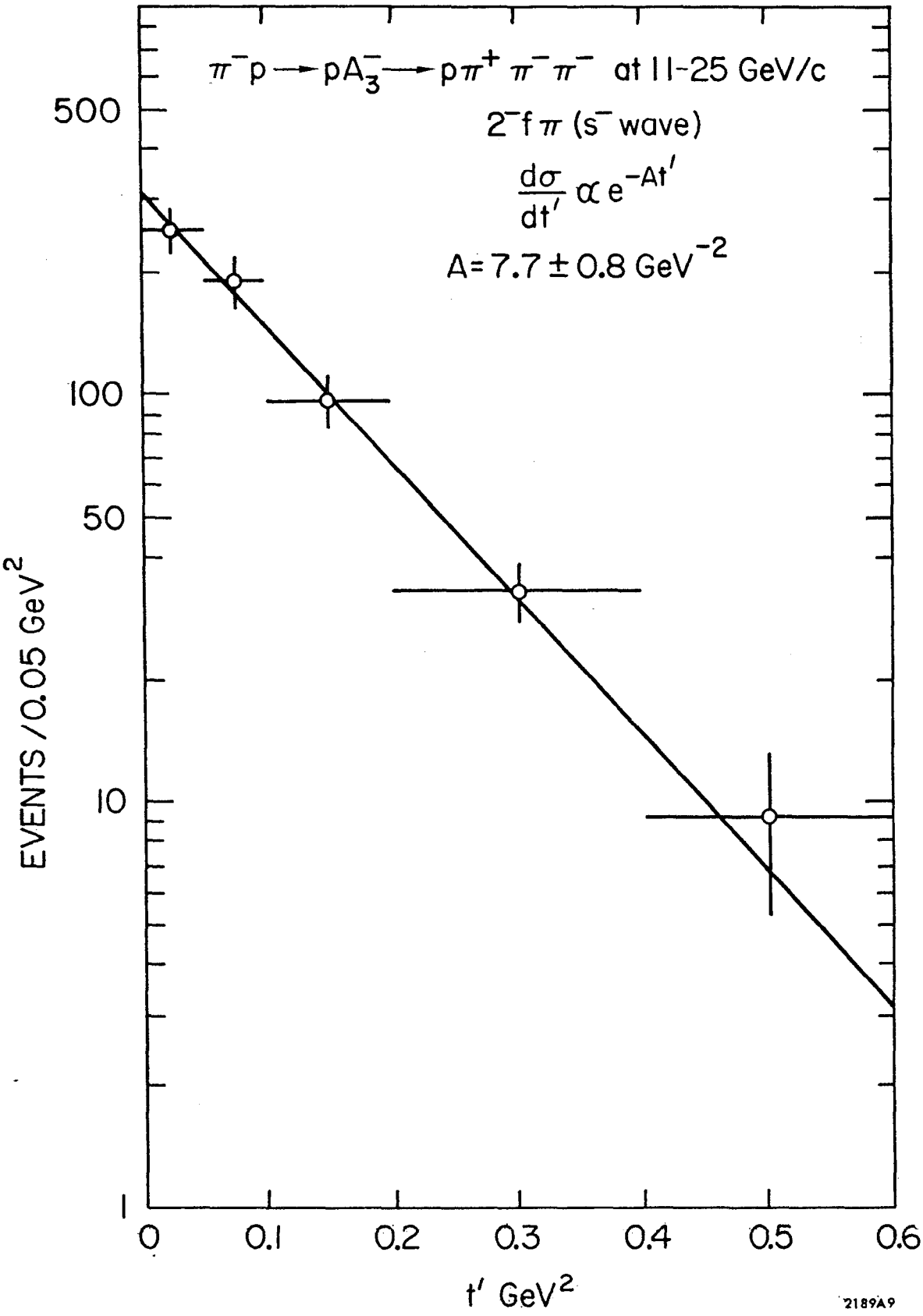

FIG. 22--The differential cross section for $\pi^- p \rightarrow A_3^- p$ averaged over the momentum region (11 - 25) GeV/c. The A_3 is defined as the 2^- spin parity amplitude for $f^0\pi$ masses in the region (1.5-1.8) GeV.

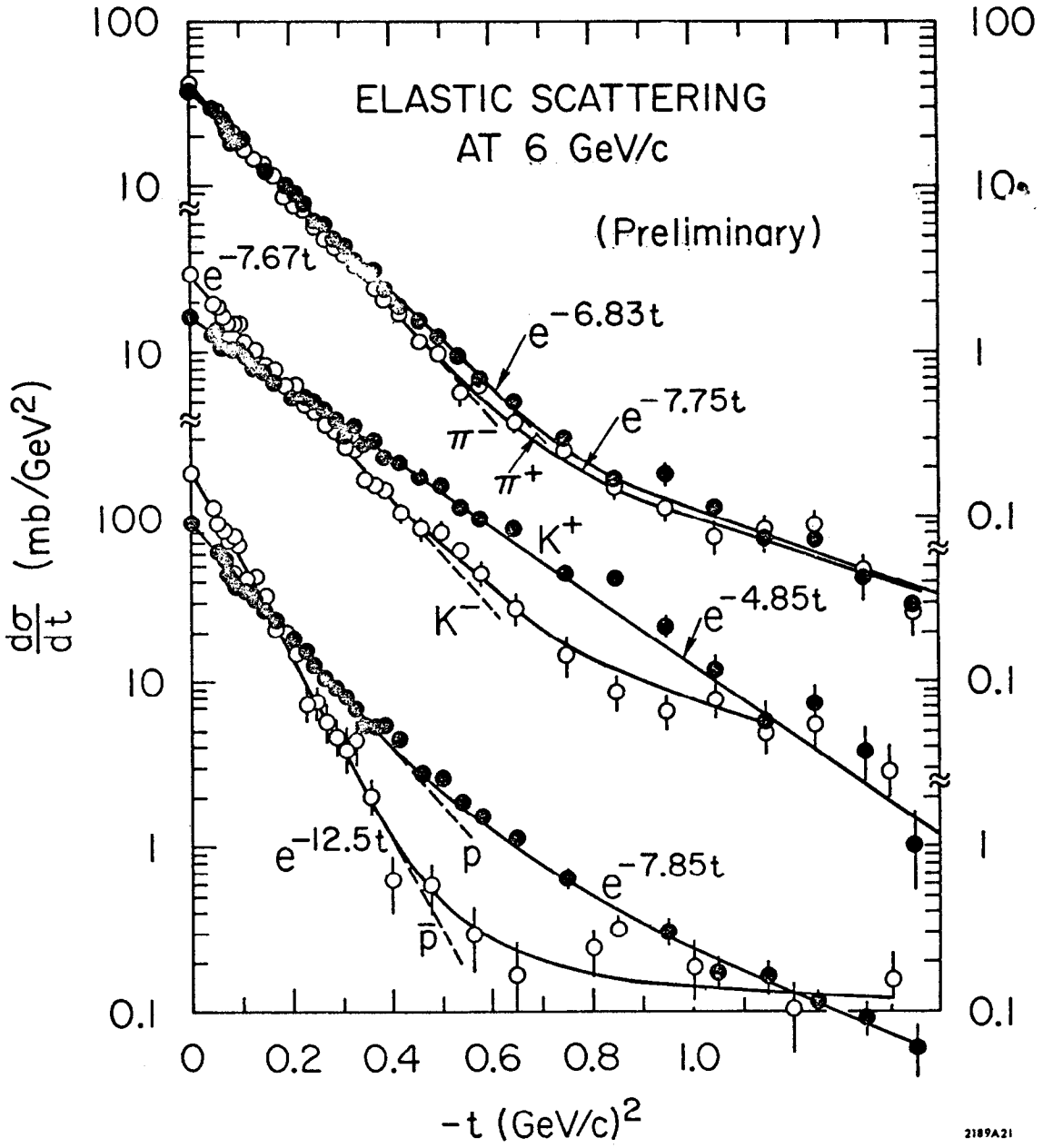

FIG. 23--Preliminary differential cross sections for $\pi^{\pm}p \to \pi^{\pm}p$, $K^{\pm}p \to K^{\pm}p$, $p^{\pm}p \to p^{\pm}p$ at 6 GeV/c, exhibiting the cross-over phenomenon for particle and antiparticle elastic scattering.

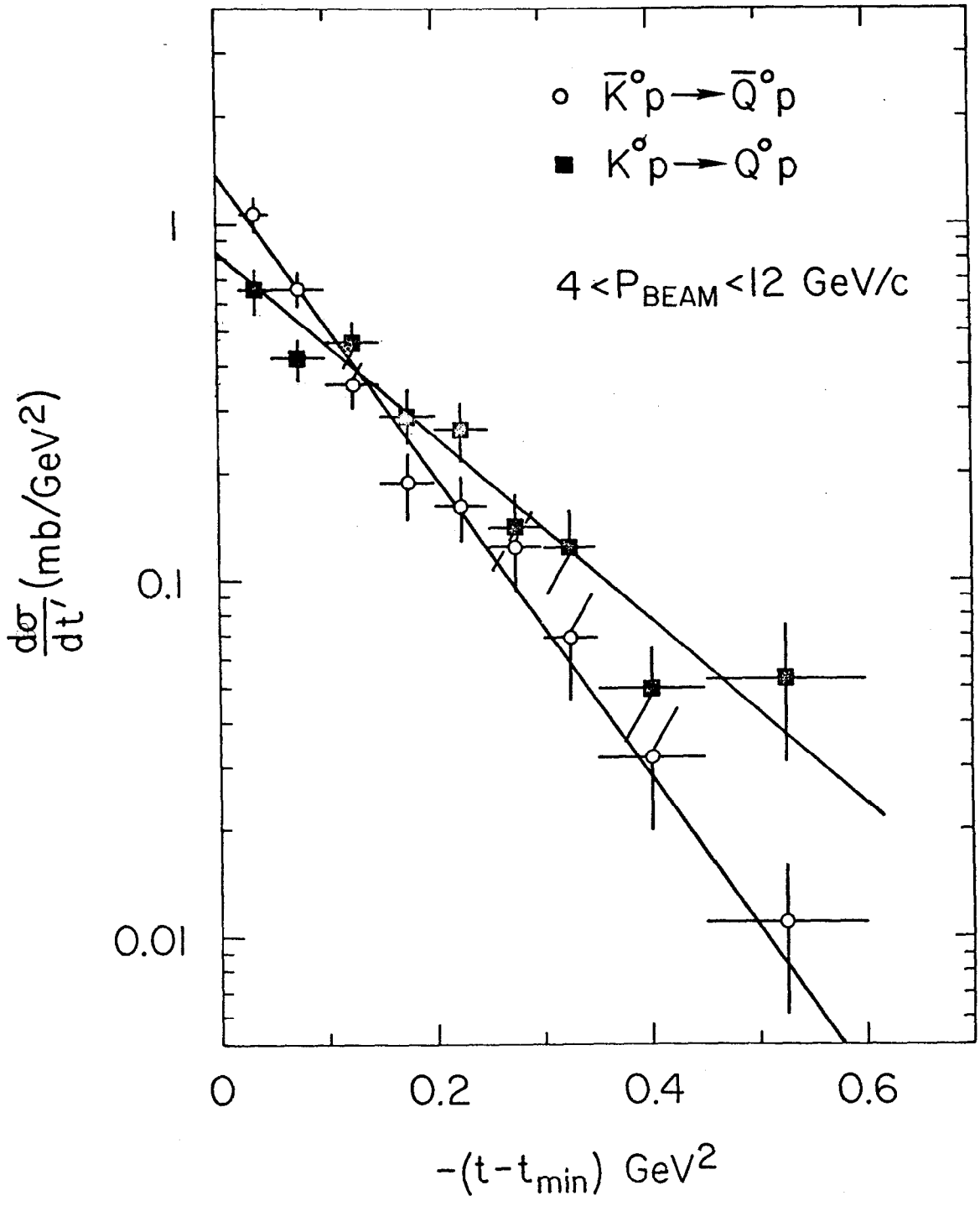

FIG. 24--Differential cross sections for $K^0p \rightarrow Q^0p$ (squares) and $\bar{K}^0p \rightarrow \bar{Q}^0p$ (circles) over the momentum range 4 to 12 GeV/c. The scale of the ordinate is determined for neutral Q mesons decaying into $K^0_S\pi^+\pi^-$. The curves result from the following exponential fits:

$$\frac{d\sigma}{dt'}(Q^0p) = 0.83 \exp(5.9\, t') \text{ mb/GeV}^2,$$

$$\frac{d\sigma}{dt'}(\bar{Q}^0p) = 1.36 \exp(9.7\, t') \text{ mb/GeV}^2.$$

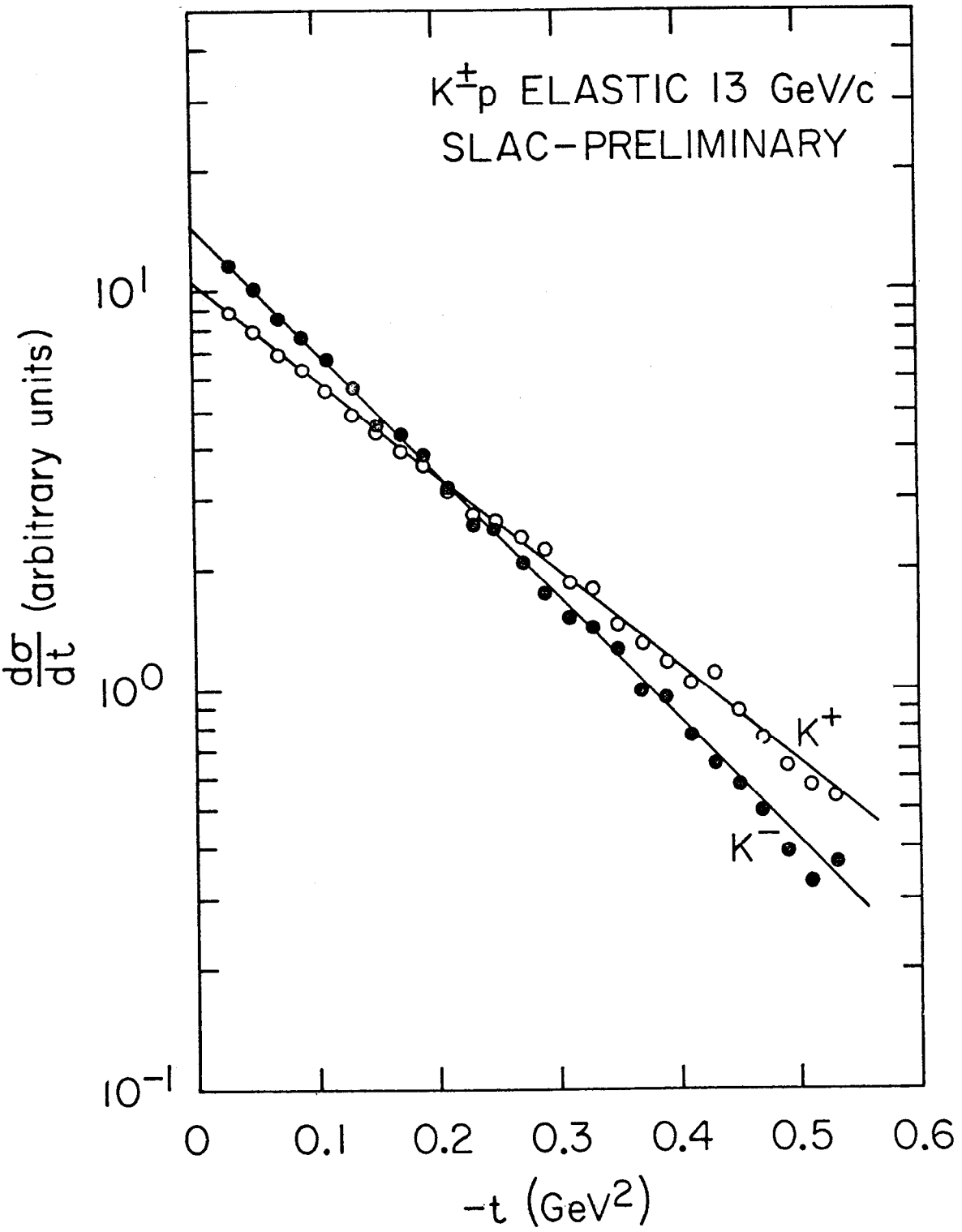

FIG. 25--The differential cross section for K^+p and K^-p elastic scattering at 13 GeV/c.

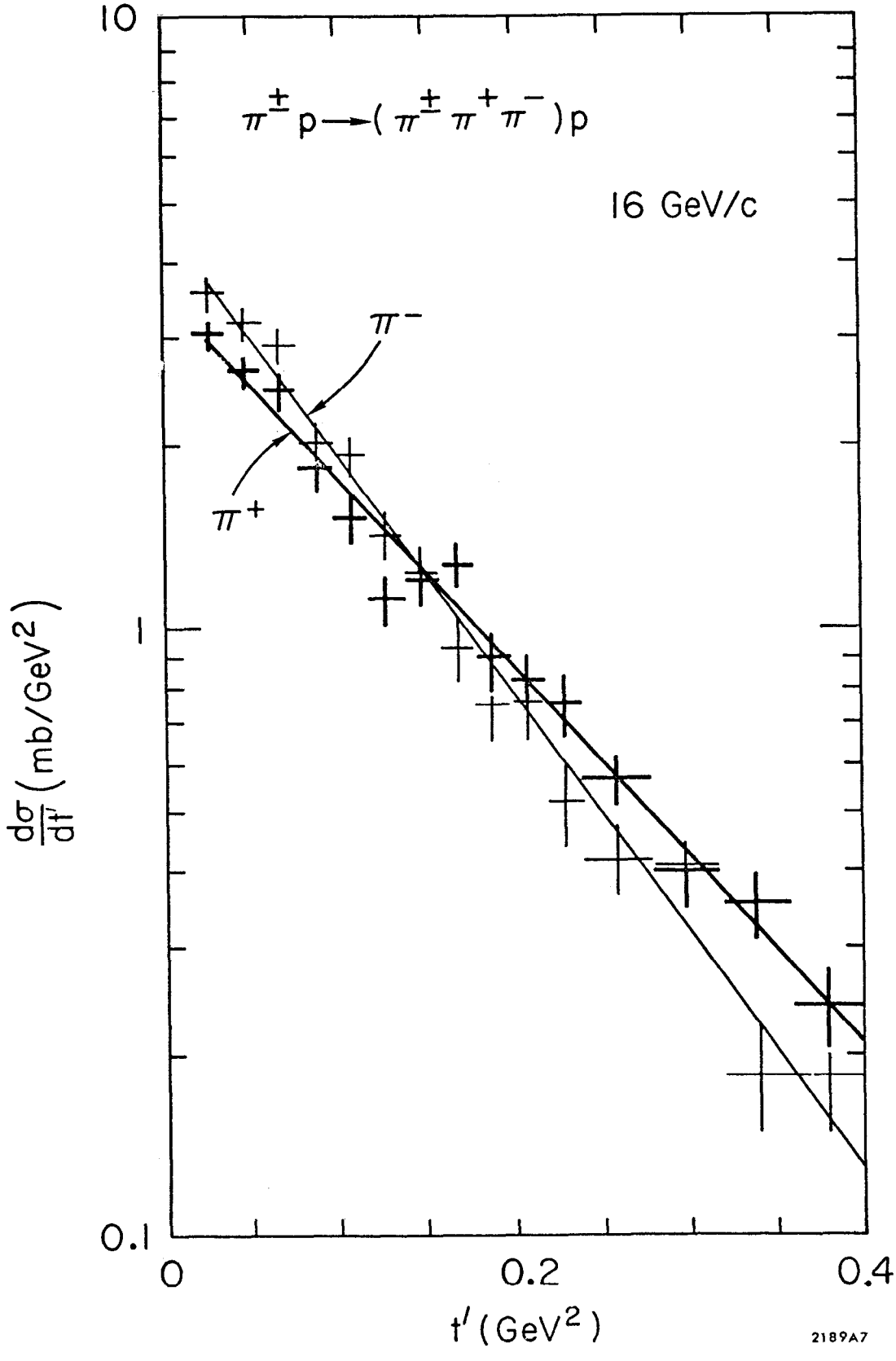

FIG. 26--The four-momentum transfer distribution, $d\sigma/dt'$, for the reaction $\pi^{\pm}p \rightarrow (\pi^{\pm}\pi^{+}\pi^{-})p$ in the pion-dissociation section.

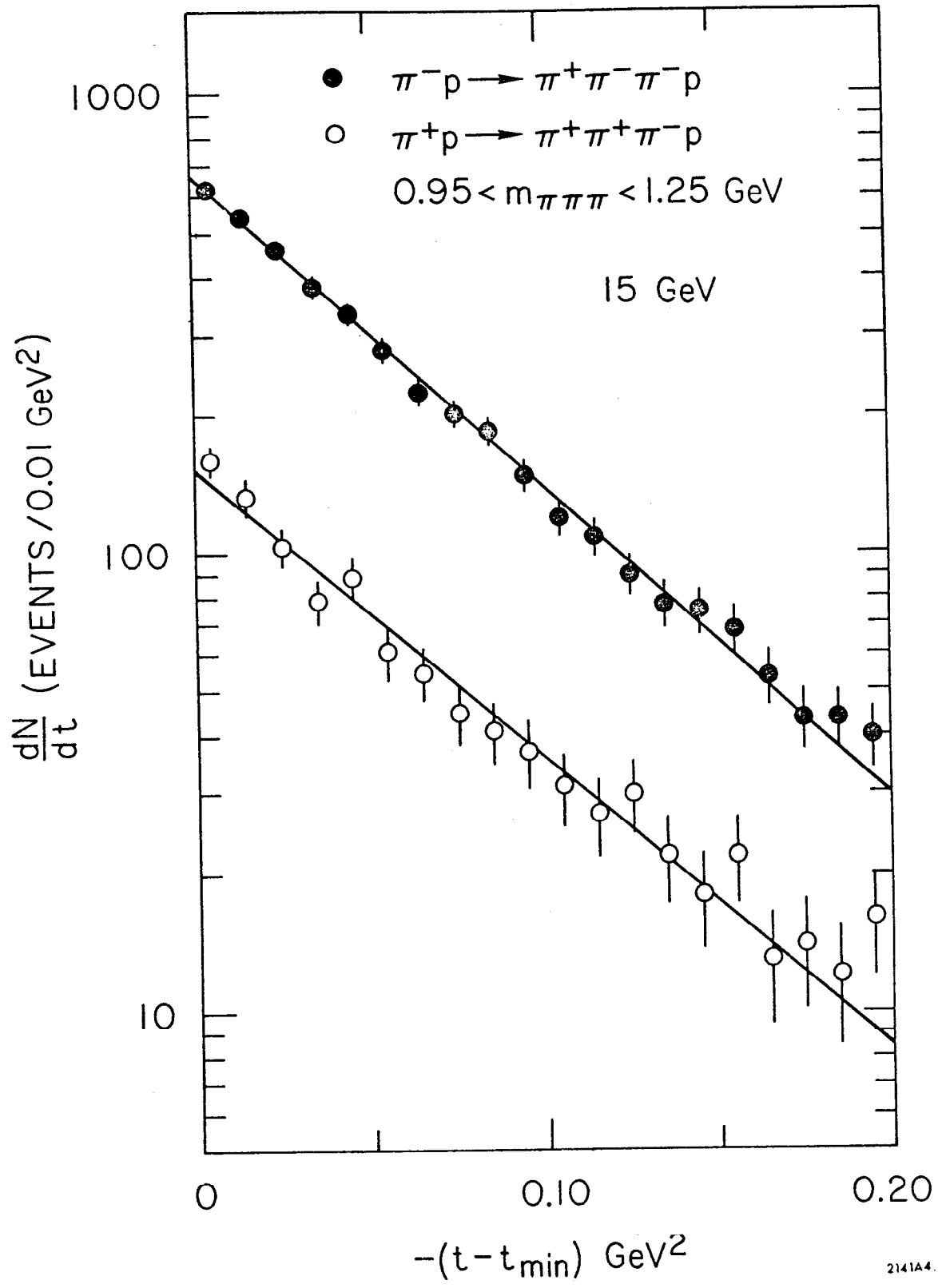

FIG. 27--Observed production angular distribution for $\pi^{\pm} p \rightarrow A_1^{\pm} p$. The curves are obtained from fits to the function $N_0 e^{bt'}$ which yield $b^+ = 14.50 \pm .73$ GeV^{-2} and $b^- = 15.59 \pm .35$ GeV^{-2}.

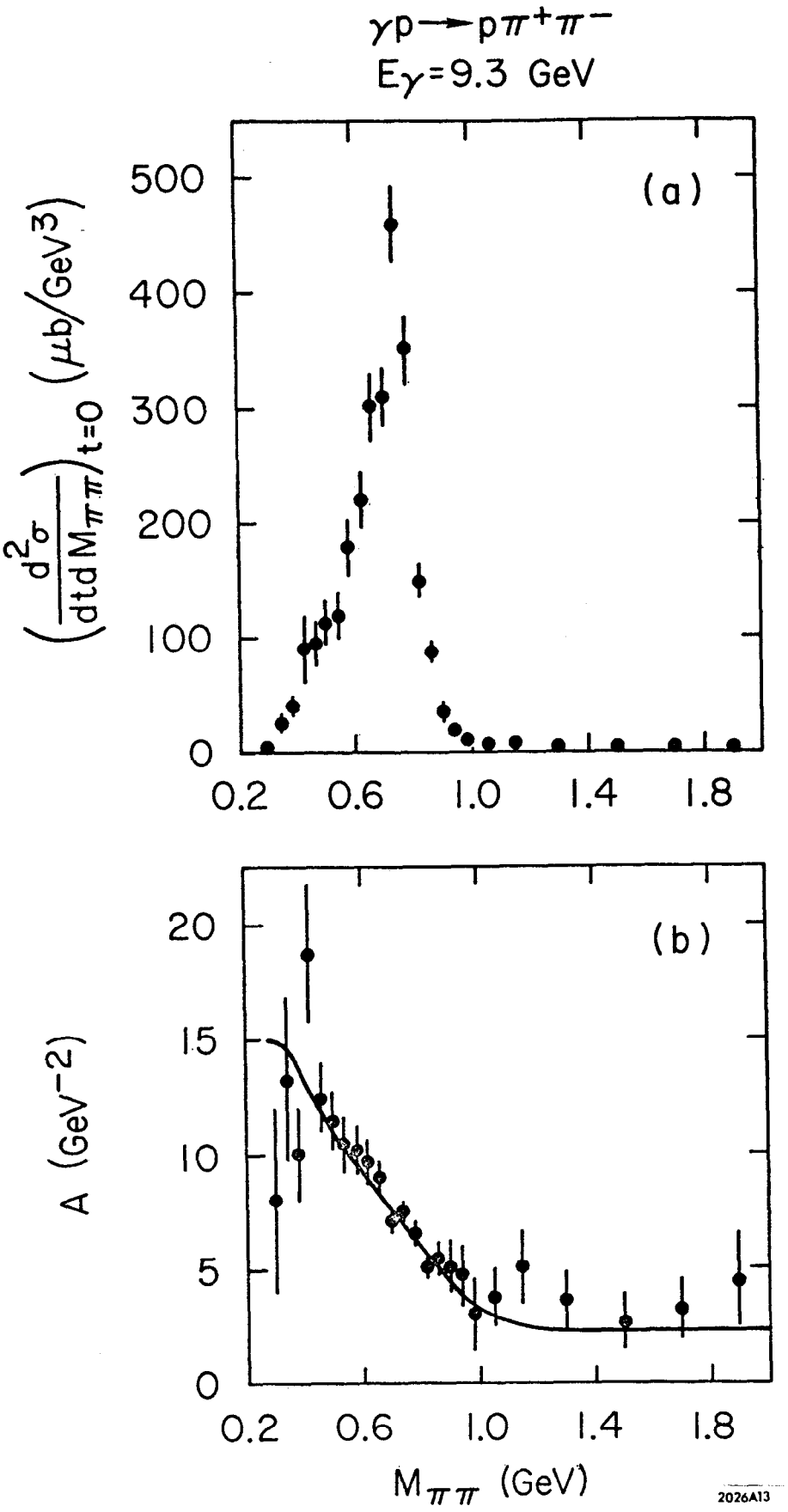

FIG. 28--Reaction $\gamma p \to p\pi^+\pi^-$ at 9.3 GeV. Results of fits of the form

$$d\sigma^2/dtdM_{\pi\pi} = d\sigma^2/dtdM_{\pi\pi\ t=0} \cdot e^{At}$$

in the interval $0.02 \leq t \leq 0.5$ GeV^2. The curve is from the Söding model.

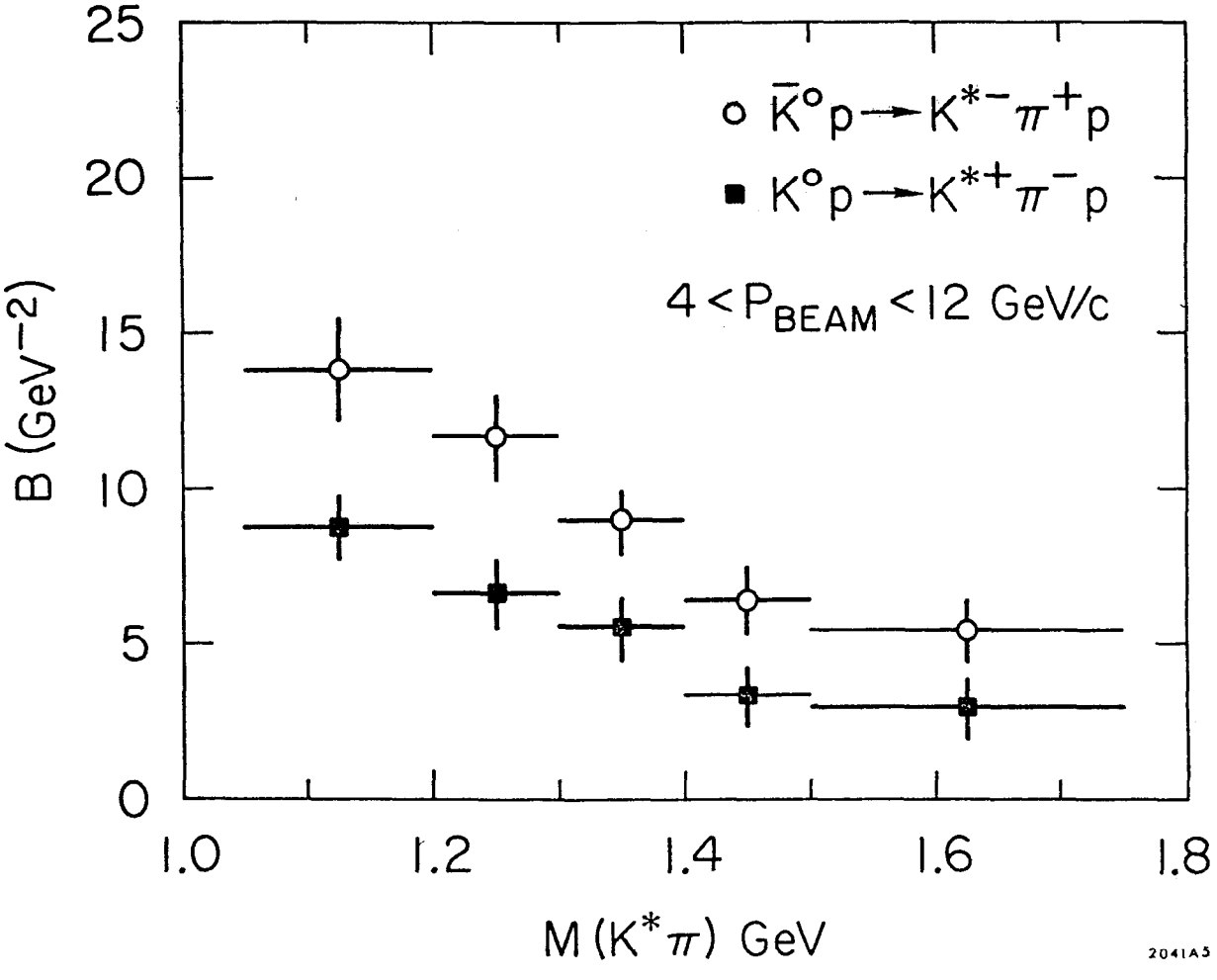

FIG. 29--Exponential slope parameter, B, averaged over the interval $4 < P_{BEAM} < 12$ GeV/c and plotted versus the mass of the $K^*(890)^+ \pi^-$ (squares) and the mass of the $K^*(890)^- \pi^+$ (circles).

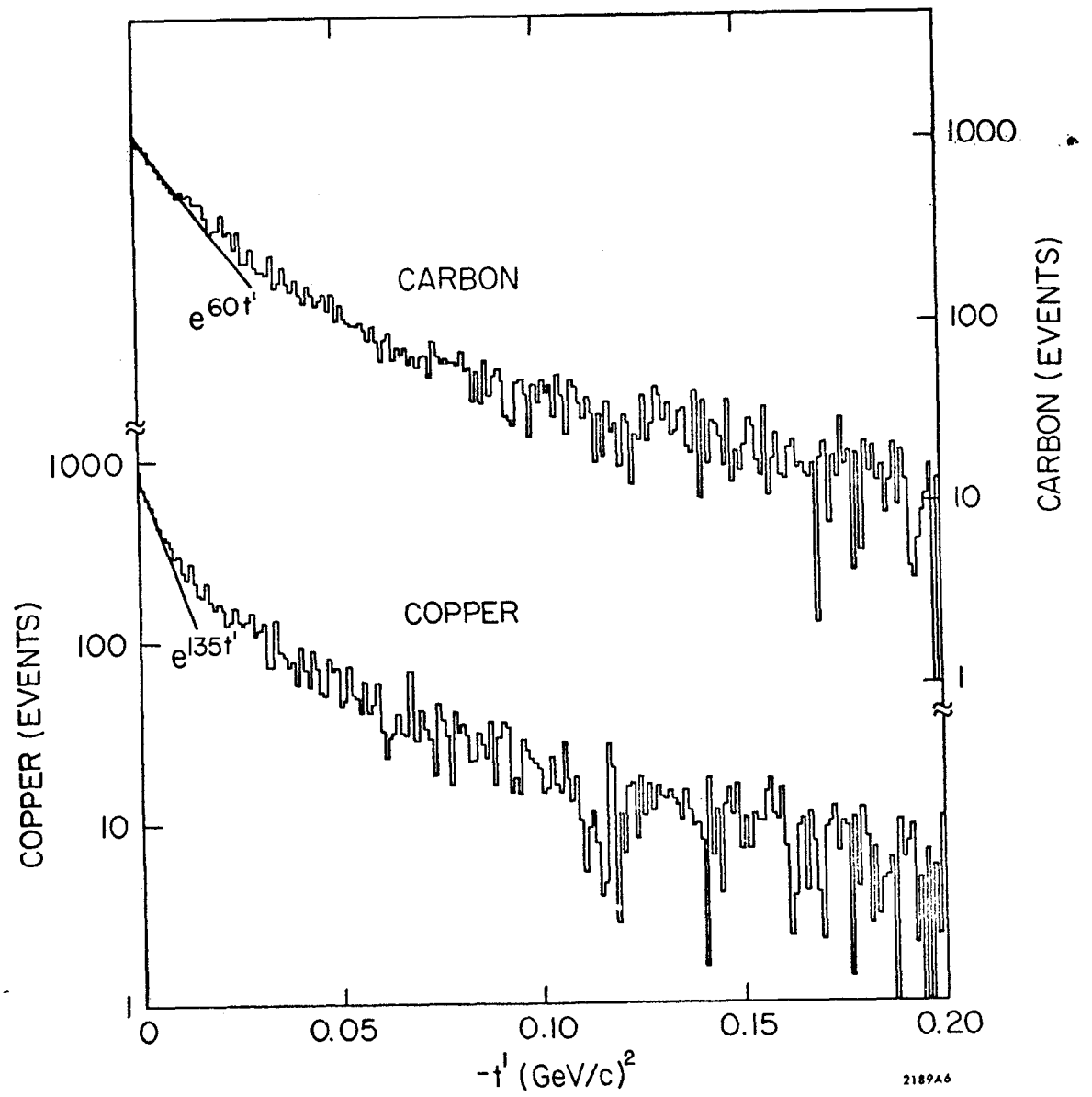

FIG. 30--Distribution of events with t' for carbon and copper targets. "Target-out" background has been subtracted. The straight line is hand-fitted to the data at small t'. Expected values of b are ≈ 53 (GeV/c)$^{-2}$ for carbon and ≈ 160 (GeV/c)$^{-2}$ for copper.

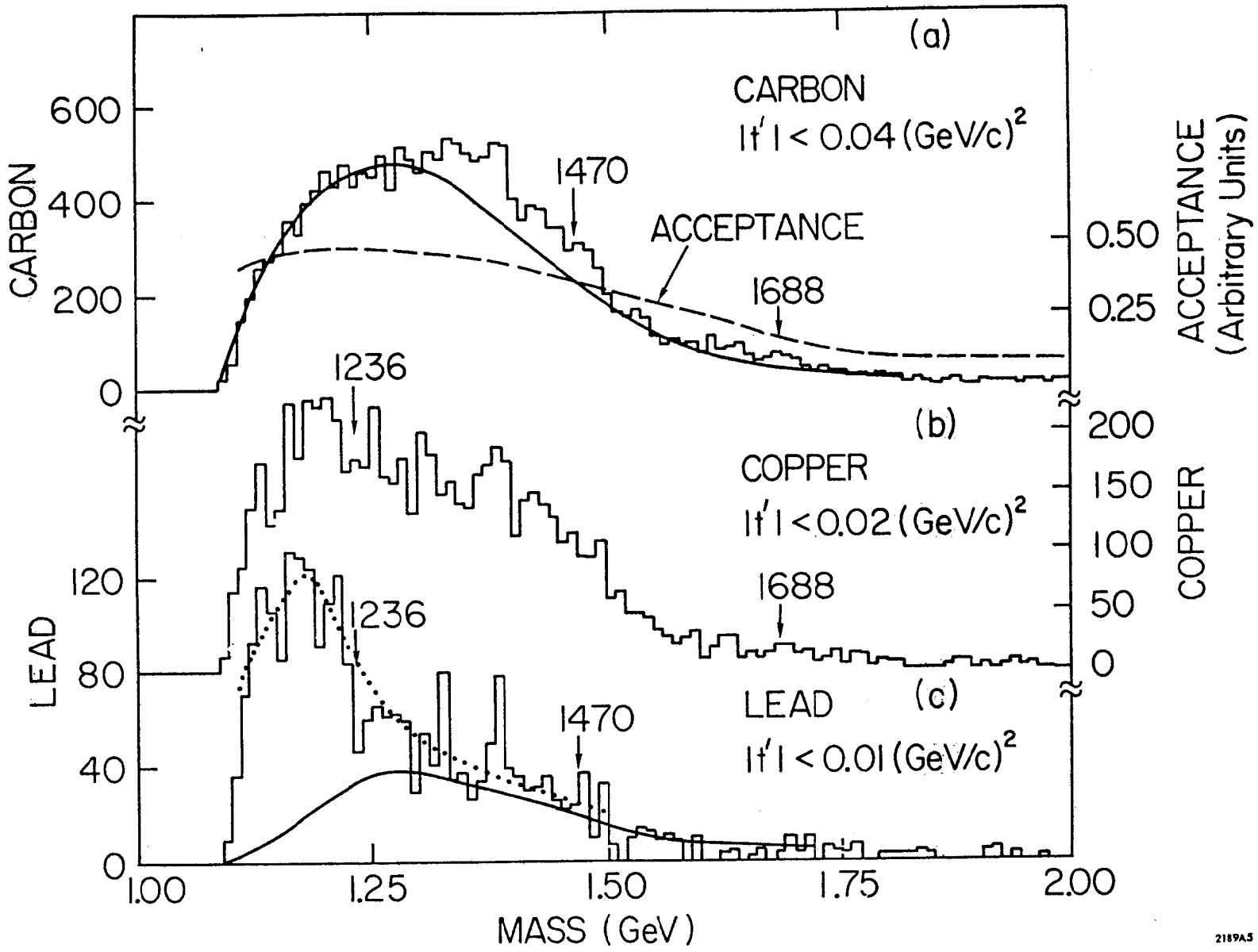

FIG. 31--Mass distributions (events per 10 MeV) for the $p\pi^-$ system observed with carbon, copper, and lead targets. The efficiency of the apparatus vs. mass, shown by the dashed curve in (a), has not been unfolded.

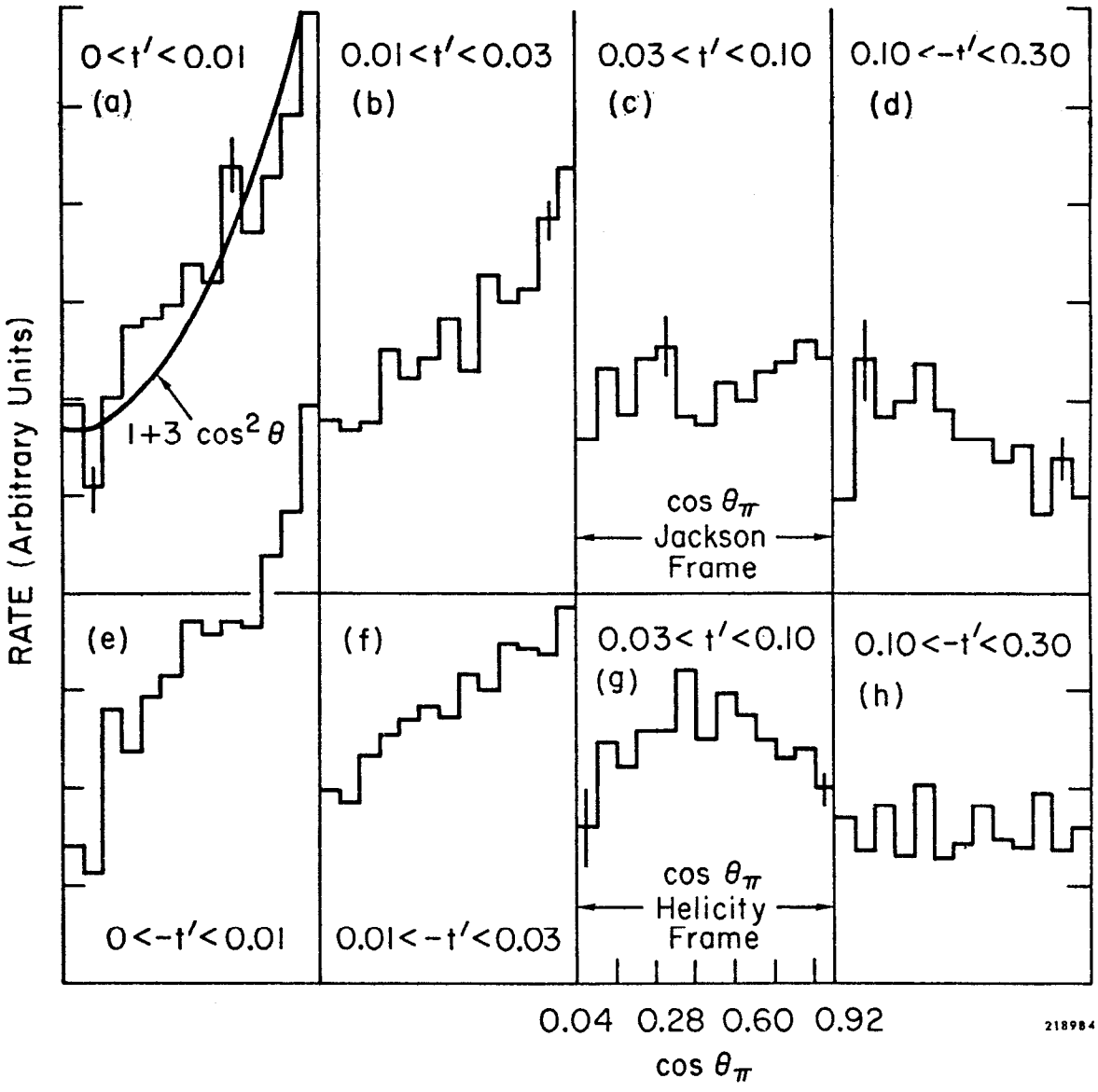

FIG. 32--Distributions in the cosine of the polar angle of the π^- in the $p\pi^-$ rest frame. (a)-(d) are for various t' bins as indicated and θ is measured in the Jackson frame. (e)-(h) are for the same t' bins with θ measured in the helicity frame. Note that all distributions only cover the angular range $-.04 < \cos\theta < 1.0$. The $p\pi^-$ invariant mass is restricted to the interval 1.10 - 1.32 GeV. The higher mass region gives similar results.

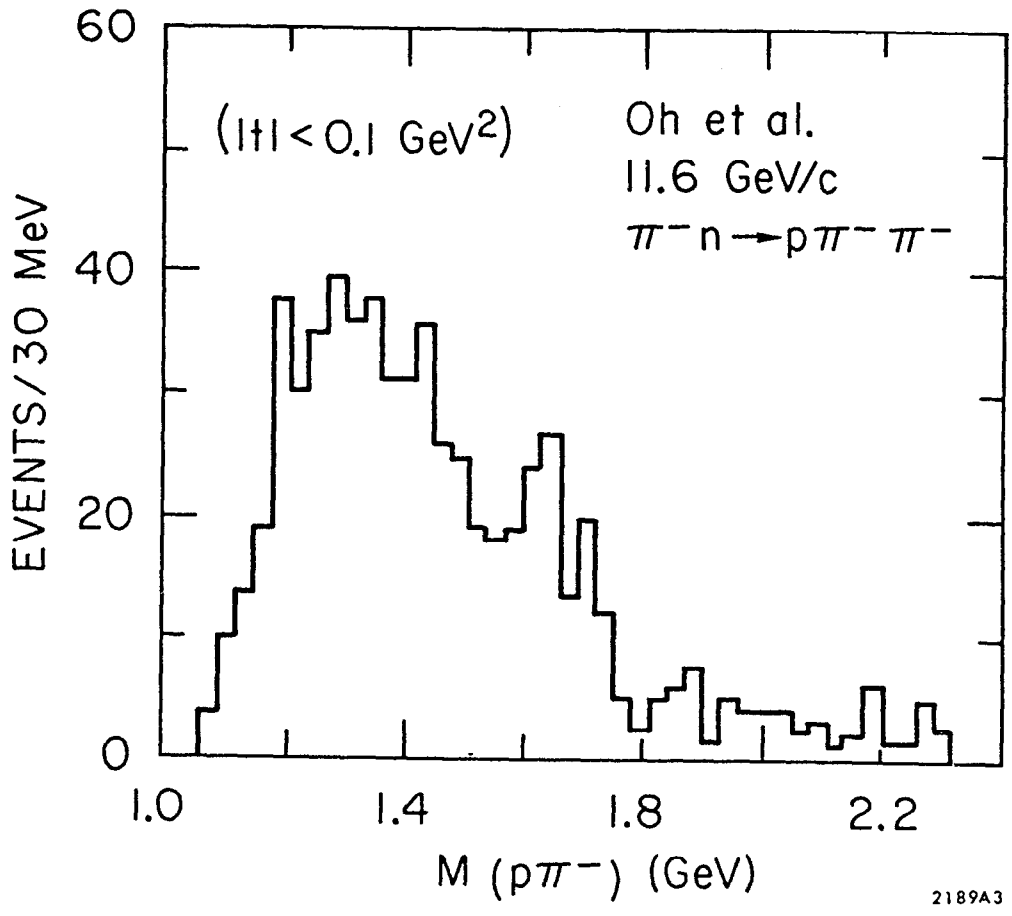

FIG. 33--The $p\pi^-$ mass distribution for the reaction $\pi^-n \to p\pi^-\pi^-$ at 11.6 GeV/c.

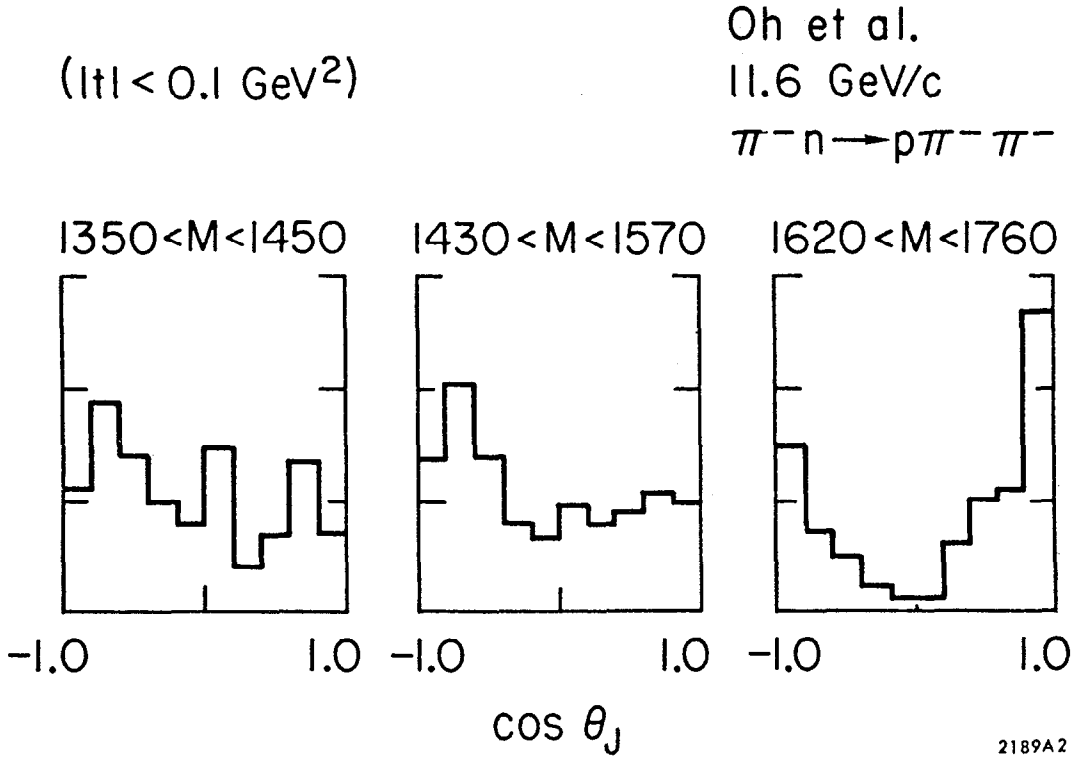

FIG. 34--The angular distribution for the $p\pi^-$ system, for three regions of $p\pi^-$ mass.

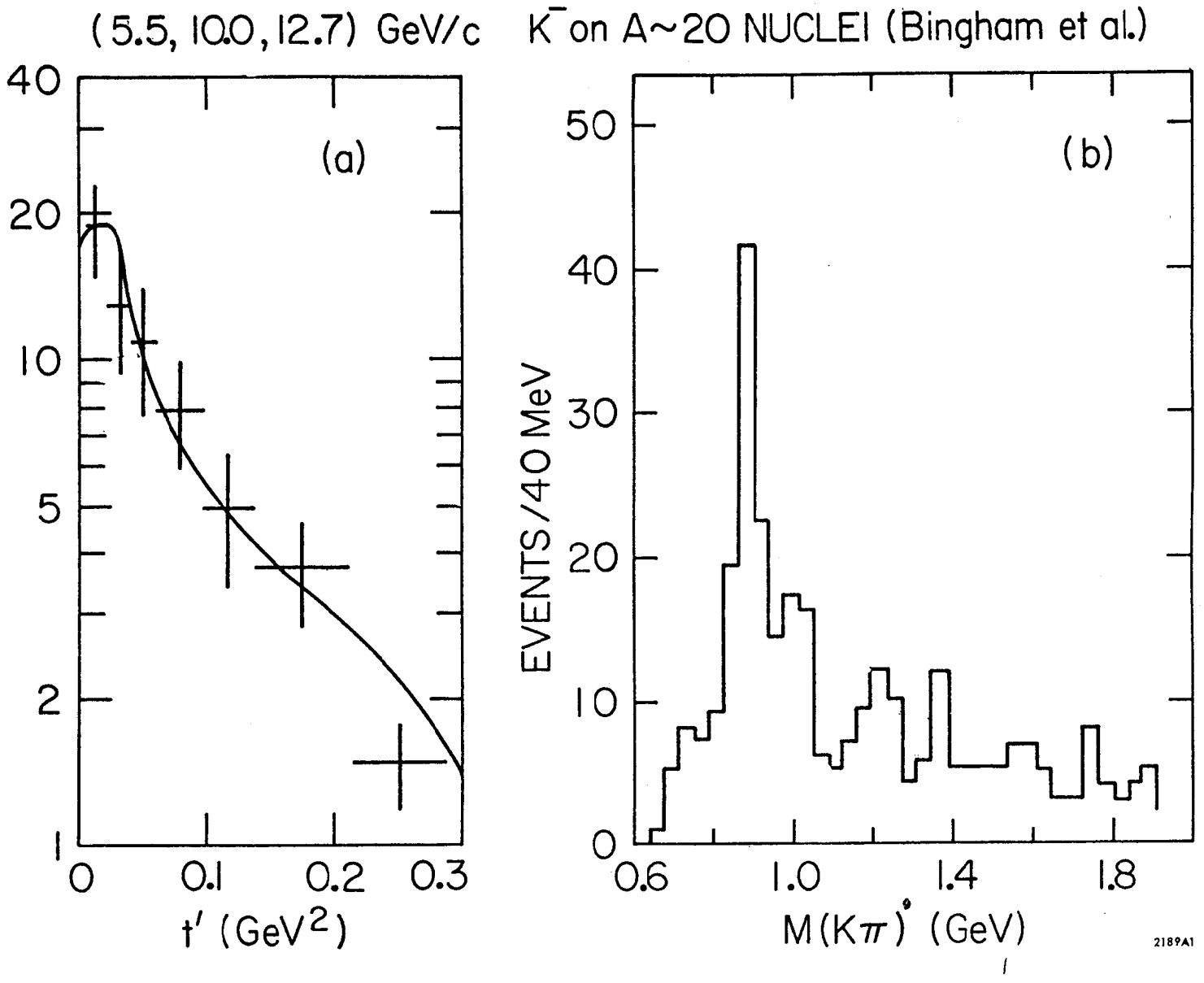

FIG. 35--The K^*_{890} production angular distribution and the $K\pi$ mass distribution from a K^- experiment at (5.5, 10.0 and 12.7) GeV/c in a heavy liquid bubble chamber.